Working Paper

Modeling Atmospheric Transport of Heavy Metals Over Europe in the 50 km Grid System

Jerzy Bartnicki and Krzysztof Olendrzyński

WP-96-141
December 1996

IIASA International Institute for Applied Systems Analysis • A-2361 Laxenburg • Austria
Telephone: +43 2236 807 • Telefax: +43 2236 71313 • E-Mail: info@iiasa.ac.at

Modeling Atmospheric Transport of Heavy Metals Over Europe in the 50 km Grid System

Jerzy Bartnicki[1] *and Krzysztof Olendrzyński*[2]

[1] DNMI - Norwegian Meteorological Institute, Oslo, Norway
[2] IIASA - International Institute for Applied Systems Analysis, Laxenburg, Austria

WP-96-141
December 1996

IIASA International Institute for Applied Systems Analysis • A-2361 Laxenburg • Austria
Telephone: +43 2236 807 • Telefax: +43 2236 71313 • E-Mail: info@iiasa.ac.at

Table of Contents

Acknowledgments

This study could not have been performed without the continuing support and assistance of William Stigliani and Stefan Anderberg, co-leaders of IIASA's Regional Material Balance Approaches to Long-Term Environmental Policy Planning (IND) Project.

We are also grateful to Josef Pacyna from the Norwegian Institute for Air Research (NILU) for his help in developing the heavy metals emission data base for 1992 in the 50 km grid system.

Abstract

Within the framework of the collaborative project between IIASA and the Norwegian Meteorological Institute in Oslo, a new version of the Heavy Metals Eulerian Transport (HMET) model has been developed.

This new version is presented in this paper, as well as the results of the model simulation for one year period of transport (1992). The main difference between the old version (here termed as HMET-150), and a new version called HMET-50, is the model grid size reduced from 150 km in the old approach, to 50 km in the latest model version. Higher spatial resolution is important for estimating atmospheric load of heavy metals to European soils.

The HMET-50 model was used to simulate atmospheric transport and deposition in Europe of arsenic (As), cadmium (Cd), lead (Pb) and zinc (Zn). Necessary emission data for this simulation were compiled at IIASA. Meteorological input for the HMET-50 model was prepared at the Norwegian Meteorological Institute in Oslo.

Maps of computed total depositions in Europe for all metals are presented. In addition, concentration maps, as well as dry and wet deposition maps, for all metals are also shown in the paper. The change of the model grid size influenced the locations of the deposition maxima. Because of the better resolution of emissions, computed concentrations are slightly closer to measured values. However, this fact has to be confirmed when more measurements for 1992 become available.

1. Introduction

Atmospheric deposition is an important source of heavy metals in European soils and forests (Prieler *et al.*, 1996). Estimation of the atmospheric deposition can be based either on model computations or measurements. Direct deposition measurements of heavy metals fluxes are expensive and difficult to make. They are performed in a limited number of locations in Europe for short time periods only. Therefore, application of the transport/deposition models is a reasonable solution of the problem.

Data on atmospheric deposition to European soils are essential for IIASA's Regional Material Balance Approaches to Long-Term Environmental Policy Planning (IND) project. The atmospheric deposition of Cd, Pb and Zn in Europe, was first calculated by Olendrzyński *et al.* (1995, 1996) for a 33-year period (1955-1987), using the simple climatological TRACE model developed at IIASA (Alcamo *et al.*, 1991; 1992). Due to various limitations of the climatological model, such as statistical representation of the transport pattern, aggregated meteorological data with low resolution and significant simplifications in the parameterizations of the deposition processes, the results of the TRACE model could be only considered as first approximations of the deposition fluxes.

Therefore, in the next step the more sophisticated Heavy Metals Eulerian Transport Model (HMET), developed by Bartnicki *et al.* 1993 and Bartnicki (1994, 1996) was used to calculate long term deposition of As, Cd, Pb and Zn in Europe. The original HMET model works in the grid system with 150 km resolution, which is compatible with the standard EMEP grid for Europe (Barret and Berge, 1996). EMEP stands for the Co-operative Programme for Monitoring and Evaluation of the Long Range Transmission of Air Pollutants in Europe. The main objective of EMEP is to service technical needs of governments and subsidiary bodies under the 1979 Geneva Convention on Long Range Transboundary Air Pollution. The HMET model is using the EMEP grid system because this is the only system with available long term, 6-hour resolution meteorological data. Using these meteorological data, simulations with the HMET model have been performed for the 10-year period: 1986 - 1995. Based on the results of these simulations, source-receptor matrices for As, Cd, Pb and Zn have been computed and then long-term depositions of these metals in Europe. A description of this study will be published in a separate journal paper.

Even though the HMET model is using maximum of emission and meteorological information that is available for a long term simulation from the impact point of view, it is desirable to have a deposition field with a better spatial resolution. This is the main reason why a new version of the HMET model, called HMET-50, has been developed within the framework of a collaborative project between IIASA and the Norwegian Meteorological Institute (DNMI). The HMET-50 model has been designed in the 50 km grid system that is a subset of the standard EMEP grid. Since meteorological data in the new grid are available only for one year, simulations with the HMET-50 have been performed only for 1992. The results of this simulation and their comparison with the HMET-150 model results are presented in this paper.

2. Description of the HMET-50 Model

A new version of the HMET model with 50 km grid resolution is very similar to the model version developed for 150 km grid. The vertical structure of the HMET-50 is shown in Figure 1. The atmosphere is represented in the model by two layers: the mixing layer and the residence layer.

The first model assumption states that heavy metals are emitted into the mixing layer. Immediately after emission, metals are well mixed in this layer so that the initial concentration is homogenous in the vertical direction below the mixing height h. The range of values for the mixing height is 200-2500 m. Metals in the mixing layer are advected horizontally with the wind field from the σ-level=0.925, which corresponds to approximately 570 m. The thickness of the mixing layer is variable in space and time depending on the current value of the mixing height. There is no exchange of metals between the residence layer and the free troposphere.

Metals are removed from the mixing layer by dry and wet deposition processes. Efficiency of the dry deposition is a function of the mixing height, terrain type and atmospheric stability. Wet deposition depends on the mixing height, precipitation intensity and the scavenging ratio. Diurnal variation of the mixing height is the main mechanism for the vertical exchange of heavy metals between the mixing layer and the residence layer parameterized by the vertical exchange flux F_e in Figure 1.

The top of the residence layer (H=3000 m) was chosen in such a way that the maximum of the mixing height is still below the top of the residence layer. Horizontal transport in the residence layer is calculated using the same wind as in the mixing layer. During transport, metals in the residence layer are only affected by wet deposition process that is parameterized in a similar way as in the mixing layer. However, the scavenging ratio is higher at this level because of the more frequent presence of clouds there.

2.1 Model equations

Four metals are taken into account in the HMET-50 model: As, Cd, Pb and Zn. Additional metal, Cu, present in the 150 km version of HMET was not included here because emissions for this metal are only available for the year 1989 and meteorological data for this particular year (in 50 km grid system) are not available. Transport of each heavy metal in two vertical layers is described in the model by a set of two transport equations (one set for each metal):

$$\frac{\partial c}{\partial t} + \frac{\partial uc}{\partial x} + \frac{\partial vc}{\partial y} = S \tag{1}$$

$$\frac{\partial c_r}{\partial t} + \frac{\partial uc_r}{\partial x} + \frac{\partial vc_r}{\partial y} = S_r \tag{2}$$

where $c(x,y,t)$ and $c_r(x,y,t)$ are the ambient concentrations of As, Cd, Pb and Zn in the mixing layer and in the residence layer respectively; $u=u(x,y,t)$ and $v=v(x,y,t)$ are

components of the velocity field from σ=0.925 level; S and S_r represent all sources and sinks of heavy metals in the mixing layer and in the residence layer respectively and include the following terms:

$$S = \left(\frac{\partial c}{\partial t}\right)_{emi} + \left(\frac{\partial c}{\partial t}\right)_{dry} + \left(\frac{\partial c}{\partial t}\right)_{wet} + \left(\frac{\partial c}{\partial t}\right)_{ex} \tag{3}$$

$$S_r = \left(\frac{\partial c_r}{\partial t}\right)_{wet} + \left(\frac{\partial c_r}{\partial t}\right)_{ex} \tag{4}$$

In Equations (3) and (4), terms on the right hand side describe the following processes:

$\left(\frac{\partial c}{\partial t}\right)_{emi}$ - emissions of heavy metals in the mixing layer,

$\left(\frac{\partial c}{\partial t}\right)_{dry}$ - dry deposition of heavy metals in the mixing lay

$\left(\frac{\partial c}{\partial t}\right)_{wet}$ - wet deposition of heavy metals in the mixing lay

$\left(\frac{\partial c}{\partial t}\right)_{ex}$ - flux of heavy metals from the mixing layer to the

$\left(\frac{\partial c_r}{\partial t}\right)_{wet}$ - wet deposition of heavy metals in the residence

$\left(\frac{\partial c_r}{\partial t}\right)_{ex}$ - flux of heavy metals from the residence layer to

The advection part of the transport equations is solved according to Bott's method (Bott, 1989a, 1989b, 1992), which compared to other algorithms gives more accurate solutions with relatively low numerical diffusion. Model equations are solved in the numerical grid system shown in Figure 2. This system consists of 18987 nodes (117 x 111) which are located in the center of the 50 km grid squares. Heavy metals emissions are estimated at each node and they represent the sum of all sources within the corresponding grid square. Meteorological data are also assigned to each node and are updated every six hours during the model run. The grid system shown in Figure 2 is compatible with the EMEP 150 km grid system used for operational modeling of long range transport of sulfur and nitrogen oxides in Europe (Eliassen and Saltbones, 1983; Barret end Berge, 1996). Compatibility means that each of 150 km grid squares is covered exactly by nine 50 km grid squares.

There are two types of lateral boundary conditions applied in the model computations. In the case of inflow, it is assumed that the air coming into the model domain does not contain heavy metals. For the outflow case, heavy metals can freely leave the model domain.

Parameterization of all sink and source terms in Equations (3) and (4) will be described in detail in the following sections.

2.2 Parameterization of heavy metals emissions

Only anthropogenic emissions are included in the inventories that served as input for the HMET-50 model. The emission source term in Equation (3) is parameterized as follows:

$$\left(\frac{\partial c}{\partial t}\right)_{emi} = (1-\alpha)\cdot\frac{Q}{h} \tag{5}$$

where $Q=Q(x,y,t)$ is the emission intensity per model grid square for each of the four metals, α is the local deposition coefficient and $h=h(x,y,t)$ is the mixing height. Unlike the previous versions of the HMET model, in the present approach, emission intensity Q is a function of time expressed as:

$$Q(x,y,t) = Q_t(t)\cdot Q_s(x,y) \tag{6}$$

where $Q_t(t)$ includes seasonal and daily variation of emissions and $Q_s(x,y)$ is the annual emission inventory in the EMEP grid, which for a given year does not depend on time. The parameterization of Q_t is different for Pb than for Ad, Cd and Zn, because for Pb approximately 80% of emissions come from road traffic and the rest from the point sources. For the remaining metals, up to 80-95% of emissions can be assigned to point sources.

Since most of As, Cd and Zn emissions are coming from industrial sources, the seasonal variation of emission was simply parameterized as a cosine function with 30% amplitude and minimum during the summer time. The same temporal parameterization is currently used in the EMEP operational models for sulfur and nitrogen oxides. Because of the industrial nature of these emissions, no diurnal variation was implemented in this case. Seasonal variation of As, Cd and Zn emissions reflects the changes in energy consumption in European countries and has to be considered as the first approach to the problem.

Lead emissions are strongly correlated with traffic intensity and therefore, temporal variation of traffic determined the Pb emission intensity as a function of time. Daily and seasonal variations of Pb emissions are now included in the model equations. Seasonal pattern is shown in Figure 3 and daily variations in Figure 4. These figures are based on the results of the GENEMIS subproject within the EUROTRAC project. The time dependent part of the emission in Equation (6) - Q_t(t) is a superposition of the seasonal pattern and a daily pattern in Figures 3 and 4.

The local deposition coefficients α are introduced in the model equations to account for more efficient deposition close to the sources. The α factor is constant for each metal and was estimated in the HMET model by computing a difference between the deposition calculated from the Gaussian model and the deposition calculated with the assumption of complete and immediate dispersion of heavy metals in the mixing layer for one model grid cell and typical meteorological conditions (Bartnicki, 1994). In the HMET-50 model, for As, Cd and Zn, the local deposition coefficient α=0.04 and for Pb, α=0.06.

2.3 Dry deposition

During transport pollutants are removed from the air by different processes of which the most important are dry and wet deposition. In the mixing layer turbulence is the main mechanism responsible for the transport of particles to the ground. For large particles, with a diameter larger than 10 μm, gravitational settling also becomes effective in transporting these particles downwards. Close to the surface many other processes (e.g. Brownian diffusion, electrostatic effect, surface properties) play an important role in dry deposition.

In the present model version, the sink term in Equation (4) representing dry deposition has the following form:

$$\left(\frac{\partial c}{\partial t}\right)_{dry} = -v_d(x,y,t)\cdot\frac{c(x,y,t)}{h(x,y,t)} \tag{7}$$

where v_d is the dry deposition velocity for each metal. The dry deposition velocity is computed by the semiempirical model of Sehmel (1980) as a function of particle size D_p, density r, surface roughness z_0 and friction velocity u_*. In the Sehmel model dry deposition velocity increases as density, surface roughness and friction velocity increase. However, deposition velocity is strongly dependent on the particle size. For particle diameter range between 0.1 and 1 μm, deposition velocity approaches minimum values, but it does not change very much. For particle diameter larger than 1 μm, the deposition velocity increases because of the stronger effect of turbulent diffusion and even more important, in this range, gravitational settling. For small particles with a diameter lower than 0.1 μm, Brownian diffusion becomes the controlling factor and deposition velocity increases with decreasing particle size. Mass Median Diameter (MMD) as obtained by Milford and Davidson (1985) has been used in the Sehmel model as a particle size D_p. The MMD values are: 1.11 μm, 0.84 μm, 0.55 μm, 1.13 μm for As, Cd, Pb and Zn respectively.

The use of MMD in the model calculations can lead to an overestimation of the long range transport of heavy metals because in reality the heaviest particles are deposited close to the emission sources and then contribute mostly to local deposition. On the other hand, according to van Jaarsveld *et al.* (1990) about 70% of the As, Cd, Pb and Zn mass is emitted as fine particles with a diameter lower than 0.95 μm. Thus, the long range transport is governed mainly by particles belonging to the fine size class.

The density of fine particles of anthropogenic origin was estimated by Watson *et al.* (1983) and confirmed by Sugimae (1986) as 1.7 g cm^{-3}. The same density value was used in the present model to calculate dry deposition velocity for heavy metals.
In the model computations, the friction velocity u_*, is updated every six hours based on routine meteorological data: turbulent stress - τ , temperature at 2 m - T_2 and surface pressure - p_s, using the following equation:

$$u_* = \sqrt{\frac{\tau}{\rho_a}} \tag{8}$$

where ρ_a is the density of air calculated from the equation of state:

$$\rho_a = \frac{p_s}{RT_2} \tag{9}$$

and R is the gas constant.

Table 1: Assumed roughness over different surfaces.

Surface type	z_0(m)
Sea	0.00001
Desert, snow	0.001
Grass	0.03
Countryside	0.25
Suburbia, cities	0.8
Woods	1.0

The last input variable for the Sehmel model is the surface roughness, z_0, which is a function of terrain characteristics and meteorological conditions. We assumed that surface roughness is constant throughout the year and varies in space only. In each of the model grid square, surface roughness can belong to one of the six different classes defined in Table 1 (following Eliassen and Saltbones, 1983). Since the original Sehmel curves (1980) were represented for $z_0<0.1$ *m*, we extrapolated them to larger values of z_0 using a logarithmic relation.

2.4 Wet deposition

Wet deposition of heavy metals is mainly caused by different forms of precipitation, including fog water deposition. In the HMET-50, only wet deposition caused by precipitation was taken into account, and fog-water was not included in the model equations, assuming that heavy metals particles are mostly of hydrophobic nature. The wet deposition process is described by the following equation in the mixing layer:

$$\left(\frac{\partial c}{\partial t}\right)_{wet} = -W \cdot P_w(x,y,t) \cdot \frac{c(x,y,t)}{h(x,y,t)} \tag{10}$$

and in the residence layer:

$$\left(\frac{\partial c_r}{\partial t}\right)_{wet} = -W_r \cdot P_w(x,y,t) \cdot \frac{c_r(x,y,t)}{H - h(x,y,t)} \tag{11}$$

where P_w is the precipitation intensity for the last six hours in the wet fraction of the grid square, W and W_r are the scavenging ratios in the mixing layer and in the residence layer respectively. The values of the scavenging ratios for each metal in the two layers are given in Table 2.

Table 2: Scavenging ratios for heavy metals in the HMET-50 model.

Layer/Metal	As	Cd	Pb	Zn
Mixing Layer	600 000	700 000	500 000	800 000
Residence layer	900 000	1 050 000	750 000	1 200 000

The scavenging ratios for all metals are 50% higher in the residence layer because of the more frequent presence of clouds in this layer.

Unlike the model version with 150 km grid, we do not take into account the wet and dry part of the grid square in the HMET-50 during precipitation event. This assumption is justified by a much smaller (9 times) area of the 50 km grid square, compared to 150 km grid square. In case of precipitation, we assume that the entire grid square is covered by rain or snow.

2.5 Exchange of heavy metals between the vertical layers

Diurnal variation of the mixing height is the main mechanism causing the exchange of heavy metals between the mixing layer and the residence layer. The basic concept is illustrated in Figure 1. The exchanged mass is parameterized by the vertical flux F_e. Assuming the flux to be positive when metals are transported from the residence layer to the mixing layer, the exchange terms in Equations (3) and (4) can be parameterized as follows:

$$\left(\frac{\partial c}{\partial t}\right)_{ex} = w_e \cdot c(h) \tag{11}$$

$$\left(\frac{\partial c_r}{\partial t}\right)_{ex} = -w_e \cdot c(h) \tag{12}$$

where $c(h)$ is the concentration at the mixing height level, either in the mixing layer or in the residence layer, depending on the sign of the entrainment velocity w_e. Since there is a discontinuity in the concentration profile at $z=h$, concentration from the residence layer is taken when $w_e>0$ and concentration from the mixing layer when $w_e<0$. When $w_e=0$, there is no exchange between the vertical layers. The entrainment velocity w_e is defined as:

$$w_e \equiv \frac{dh}{dt} - \overline{w}_h = \frac{\partial h}{\partial t} + u\frac{\partial h}{\partial x} + v\frac{\partial h}{\partial y} - \overline{w}_h \tag{13}$$

where w_h is the mean vertical velocity at $z=h$.

2.6 Remarks about model validation

The HMET-50 has been preliminary validated by comparing its results for 1992 with the available measurement data. The main problem with this direct validation was a small number of measurements. Therefore, the results of the HMET-50 were also compared with the results of HMET-150, which in turn, were validated with a much larger measurement data set. Spatial pattern of computed concentration and deposition fields was very similar for both model versions. The main differences could be observed close to large emission sources. In these places, HMET-50 performed better than HMET-150 because of the better resolution of the emission data. Maxima computed with the HMET-50 model were closer to measured values than those computed with the HMET-150 model. This indicates that better spatial resolution improves the model performance as long as emission data with better spatial resolution are available.

3. Emission Data for Heavy Metals

Anthropogenic emission inventories for As, Cd, Pb and Zn have been used in the HMET-50 model simulations for 1992. These inventories in the 50 km grid system have been developed at IIASA (Olendrzyński et al., 1995; 1996) based on the list of point source emissions prepared by Pacyna (1996). Contributions from individual point sources were aggregated for each grid cell. Emissions from area sources (e.g. traffic) were available only as country totals. They were distributed among the model grid squares based on the population density data available for the EMEP grid system.

3.1 As emissions in Europe in 1992

Total atmospheric emissions of As from all European countries were 2345.3 tons in 1992. Point sources dominated over area sources. The ratio of point to all sources was 76%.

A map with the spatial distribution of As emissions in 1992 is shown in Figure 5. Local maximum, 155.4 x 10^3 kg, of annual As emissions was located in northwest Russia, close to the Finnish and Norwegian border (model grid square (50,90)). Two point sources, zinc smelters Severonickel - Monchegorsk and Zapolarnyj - Nickel were the major contributors to As emissions from this model grid square.

The large sources in northwest Russia were rather isolated. A large part of Europe was covered by small As sources with emissions below 1 ton per model grid. Many large sources of As were located in the so called Black Triangle and Upper Silesia (BTUS) Regions in Central Europe.

3.2 Cd emissions in Europe in 1992

Total atmospheric emissions of Cd from all European countries were 799 tons in 1992. As in the case of As, point sources dominated over area sources also for Cd and the ratio of point to all sources was 67%.

A map with the spatial distribution of Cd emissions in 1992 is shown in Figure 6. Local maximum, 55.72 x 10^3 kg, of annual Cd emissions was located in the southern part of the Russian Federation (Europe), in the model grid square (110,83). One large point source, zinc smelter Ordzonikidze was the major contributor to Cd emissions from this model grid square.

Like in the case of As, a large part of Europe was covered by small Cd sources with emissions below 0.1 ton per model grid. Many large sources of Cd were in the BTUS Region and in the UK.

Compared to emission distribution in the 150 km grid system maximum location has moved from the eastern part of Russia, to close to the Ural mountains. Even though emissions in the 50 km grid were smaller in this region, their sum over nine grid squares was larger than the identical sum in Southern Russia. In general, location of maximum is dependent on the numerical grid resolution.

3.3 Pb emissions in Europe in 1992

Total atmospheric emissions of Pb from all European countries were 56606.7 tons in 1992. Contrary to As and Cd, area sources dominated over point sources in Pb European emissions and the ratio of point to all sources was only 21%.

A map with the spatial distribution of Pb emissions in 1992 is shown in Figure 7. Local maximum, 606.89 x 10^3 kg, of annual Pb emissions was located in the southern part of the Russian Federation (Europe), in the model grid square (110,83). In addition to local traffic, one large point source, zinc smelter Ordzonikidze was the major contributor to Pb emissions in this model grid square.

Contrary to As and Cd case, distribution of Pb emissions over Europe was more uniform. Most of Europe was covered by Pb sources larger than 10 tons per grid. Large area sources of Pb were located in Russia around Moscow because of large traffic intensity in this region and common use of leaded gasoline. In the 150 km grid system maximum of Pb emissions was different than in 50 km grid and was located in the model grid square that includes Moscow.

3.4 Zn emissions in Europe in 1992

Total atmospheric emissions of Zn from all European countries were 29524.4 tons in 1992. Even more than in the case of As and Cd, point sources dominated over area sources for Zn emissions and the ratio of point to all sources was 86%.

A map with the spatial distribution of Zn emissions in 1992 is shown in Figure 8. Local maximum, 1818.1 x 10^3 kg, of annual Zn emissions was located in the southern part of the Russian Federation (Europe), in the model grid square (110,83). One large point source, zinc smelter Ordzonikidze was the major contributor to Zn emissions from this model grid square.

Since point sources dominate for Zn, distribution of Zn emissions over Europe was non uniform and patchy. However, many larger sources of Zn were located in the BTUS Region, Germany, Benelux countries and in the UK.

In the case of Zn, maxima in the 150 km and 50 km grids were located at the same place in the southern part of the Russian Federation.

4. Meteorological Input Data

Meteorological input data for 1992 were compiled at the Norwegian Meteorological Institute in Oslo, Norway. Meteorological elements that were used as input into the HMET-50 model are summarized in Table 3. The NWP acronym in Table 3 refers to the Numerical Weather Prediction model HIRLAM (Haugen and Mitbo, 1995) which is run routinely at the Norwegian Meteorological Institute.

Table 3: Meteorological input data for the HMET-50 model.

Symbol	Meteorological parameter	Level	Input interval	Main purpose of use	Source
(u,v)	Advective wind	$\sigma = 0.925$ $z = 570$ m	6 hours	Horizontal transport	NWP model
h	Mixing height	Above the surface	12 hours (00, 12 UTC)	Mixing layer	Analysis
p	Precipitation in the grid square	Surface	6 hourly accumulated	Wet deposition	NWP model + analysis
p_s	Surface pressure	$\sigma = 1$	6 hours	Air density	NWP model
T_2	Temperature	$z = 2$m	6 hours	Air density	NWP model
τ	Turbulent stress	Surface	6 hours	Friction velocity	NWP model
C	Cloud cover	Free troposphere	6 hours	Wet deposition	NWP model
w	Vertical velocity	$\sigma = 0.925$	6 hours	Entrainment velocity	NWP model

There is one additional remark to Table 3. Precipitation amounts from the NWP-model may give an underestimation of the true value, due to the effect of "spin up" from the short time forecast of the NWP model. The NWP-model was only used

for land. Over the sea, analyzed precipitation amounts were used as input for the HMET-50 model. Because of the sparse meteorological measurement network in some parts of Russia, there is an underestimation of the precipitation amount on the right hand side border of the model domain, due to interpolation. This may lead to underestimation of the wet deposition in this region.

5. Model results for 1992

From an application point of view, the most important results of the HMET-50 simulations are computed total depositions of heavy metals. However, for general purposes it is also interesting to examine computed concentration fields.

5.1 Annual total depositions of heavy metals

Total deposition in the HMET-50 model was calculated as a sum of dry, wet and local deposition. Computed total deposition fields are shown in Figures 9, 10, 11 and 12 for As, Cd, Pb and Zn, respectively. For all metals maxima of computed total depositions are located exactly in the same grid square as maxima of emissions.

For As, apart from the local maximum located in the Kola Peninsula in northeast Russia, areas with high As deposition were located in the BTUS region. Similar tendencies for high level depositions in the BTUS region can be also observed for Cd and Zn. For Pb, the Moscow region was significantly effected by atmospheric deposition. The values of computed total deposition maxima and their locations in the model grid system are summarized in Table 4.

Table 4: Maxima of computed total depositions and their locations.

Metal	Maximum (*in mg/m^2*)	Model grid location (i,j)	Geographical region
As	18.41	(50,90)	Kola Peninsula
Cd	6.31	(110,83)	Eastern part of the Russian Federation
Pb	81.31	(110,83)	
Zn	223.82	(110,83)	

Compared to depositions of Pb for 1985, computed earlier with the HMET model (Bartnicki, 1994) with 150 km resolution, there is a significant change in the total deposition pattern for 1992 in the 50 km grid system. In 1985, Western Europe was slightly more effected by total Pb deposition than the eastern part of the continent. In 1992, there is more Pb deposition in Eastern Europe.

For all metals, wet deposition processes are more effective than dry deposition. Maps of wet depositions are shown in Figures 13, 14, 15 and 16 for As, Cd, Pb and Zn, respectively. Corresponding maps of dry depositions for As, Cd, Pb and Zn are shown in Figures 17, 18, 19 and 20, respectively. Maxima of dry and wet

depositions are located in the same grid squares as maxima of total deposition for each metal.

5.2 Mean annual concentration fields

Maps of computed mean annual concentration fields for As, Cd, Pb and Zn are shown in Figures 21, 22, 23 and 24. Compared to deposition maps, and especially to emission maps, concentration patterns are more smooth. This is because dry deposition was strongly affected by isolated, single emission sources and wet deposition was mostly influenced by the irregular precipitation patterns. On the other hand, concentrations were not so sensitive to emissions and precipitation, and in addition, they were diffused by the effect of the vertical exchange of heavy metals between the mixing layer and the residence layer.

6. Conclusions

For impact studies one obvious advantage of using the HMET-50 model instead of the 150 km version of the HMET model is better spatial resolution of computed deposition fields of heavy metals. Spatial resolution of computed depositions (also concentrations) is exactly nine times better because on model grid square with 150 km size includes nine grid squares with 50 km grid size.

In this study, simulations with the HMET-50 model were performed for 1992 for four metals: As, Cd, Pb and Zn. Analysis of the results led to the following conclusions:

- Location of the local maxima of emissions are dependent on the numerical grid resolution. A significant difference between the locations of the emission maxima in 150 and 50 km grid system have been found. Higher spatial resolution of the model grid gives a better representation of the large point sources of heavy metals. On the other hand, more detailed and improved emission inventories are required.

- Better spatial resolution requires also improved meteorological data. At present, meteorological input data in the 50 km grid system exist only for 1992 (recently they are also available for 1995). From now on, these data will be available for each year.

- For computed total depositions of heavy metals, deposition maxima are located in the same grid squares as emission maxima. For computed concentrations, maxima of Cd, Pb and Zn are in the same grids as emissions, however for As, locations of emission and concentration maxima were different.

- For As, Cd and Zn, significant depositions occurred in the BTUS region in Central Europe. For Pb large depositions values were in Russia in the Moscow region. In general, total deposition of Pb in 1992 was larger in Eastern than in Western Europe.

- Concerning wet and dry deposition, wet deposition processes are more effective in removing heavy metals from the atmosphere.

In summary, the most important products of this study were total deposition fields for As, Cd , Pb and Zn in Europe, in the 50 km grid system. These computed deposition fields have been already used by the IND project to estimate atmospheric load of heavy metals to the soil.

References

Alcamo J., Bartnicki J. and K. Olendrzyński. (1991) Modelling heavy metals in Europe's atmosphere: a combined trajectory-climatological approach. In *Air Pollution Modelling and its Application* VII (edited by van Dop H. and Steyn D.), pp. 389-398. Plenum Press, New York.

Alcamo J., Bartnicki J., Olendrzyński K. and J.Pacyna. (1992) Computing heavy metals in Europe's atmosphere-I. Model development and testing. *Atm. Env.* **26A,** 3355-3369.

Barret K. and E. Berge (eds.) (1996). Transboundary air pollution in Europe. MSC-W Status Report 1996. EMEP/MSC-W Report 1/96. Meteorological Synthesizing Centre - West, Oslo, Norway.

Bartnicki, J. (1994). An Eulerian model for atmospheric transport of heavy metals over Europe: Model description and preliminary results. *Water, Air and Soil Pollution*, **75:** 227-226.

Bartnicki, J. (1996). Computing atmospheric transport and deposition of heavy metals over Europe: country budgets for 1985. *Water, Air and Soil Pollution*, **92:** 343-373.

Bartnicki, J., Modzelewski, H., Szewczyk-Bartnicka, H., Saltbones, J., Berg, E. and A.Bott. (1993). An Eulerian model for atmospheric transport of heavy metals over Europe: Model development and testing. Det Norske Meteorologiske Institute, Report No. 117.

Bott A. (1989a). A positive definite advection scheme obtained by nonlinear renormalization of the advective fluxes. *Monthly Weather Review*, **117**: 1006-1015.

Bott A. (1989b). Reply. *Monthly Weather Review*, **117**: 2633-12636.

Bott A. (1982). A positive definite advection scheme for use in long range transport models: extension to monotonicity. In Air Pollution Modeling and Its Application VIII (H. van Dop and G. Steyn eds.), pp. 695-702, Plenum Press, New York.

Eliassen A. and J. Saltbones (1983). Modelling long-range transport of sulphur over Europe: a two year model run and some model experiments. *Atmospheric Environment* **17**, 1457-1473.

Haugen J.E and K.H. Mitbo (1995). Det operasjonelle HIRLAM systemet ved DNMI. (In Norwegian). DNMI Technical Report . Norwegian Meteorological Institute, Oslo, Norway.

van Jaarsveld J.A., van Aalst and D Onderlinden (1990). Deposition of metals from the atmosphere to The North Sea: model calculations. Report 842015002, National Institute for Public Health and Environmental Protection (RIVM), Bilthoven, The Netherlands.

Milford J.B. and C. Davidson (1985). The sizes of particulate trace elements in the atmosphere - a review. *Journal of the Air Pollution Control Association* **35(12)**, 1249-1260.

Olendrzyński, K., Anderberg S., Bartnicki J., Pacyna J. and Stigliani W. 1995. Atmospheric Emissions and Depositions of Cadmium, Lead and Zinc in Europe During the Period 1955-1987. IIASA Working Paper WP-95-35.

Olendrzyński, K., Anderberg S., Bartnicki J., Pacyna J. and Stigliani W. 1996. Atmospheric Emissions and Depositions of Cadmium, Lead and Zinc in Europe During the Period 1955-1987. *Environmental Reviews* (in print).

Pacyna J.M. (1991) Emission factors for atmospheric Cd, Pb and Zn emissions for major source categories in Europe during 1950-1985. Norwegian Institute for Air Research, NILU OR: 30/91.

Pacyna J.M. (1994) Emissions of heavy metals in Europe. In Proc. EMEP Workshop on European Monitoring, Modelling and Assessment of Heavy Metals and POPs, Beekbergen, The Netherlands, May 3-6, 1994.

Pacyna, J.M. (1996) Atmospheric emissions of heavy metals for Europe. A final report for the International Institute for Applied Systems Analysis.

Pacyna J.M. and J. Münch (1988) Atmospheric emissions of arsenic, cadmium, mercury and zinc in Europe in 1982. Norwegian Institute for Air Research, NILU OR: 17/88.

Sehmel G.A. (1980) Particle and gas dry deposition: a review. *Atmospheric Environment* **14,** 983-1011.

Prieler S., Smal H. Olendrzyński K., Anderberg S. and W. Stigliani (1996). Cadmium, zinc and lead load to agricultural land in the upper Oder and Elbe Basins during the period 1955-1994. IIASA WP-96-30. International Institute for Applied Systems Analysis, Laxenburg, Vienna.

Sugimae A (1986). Characterization of trace metals compounds in the atmosphere in terms of density. In J.O Nriagu and C.I Davidson (eds.), *Toxic Metals in the Atmosphere*. John Wiley & Sons.

Watson J.G., Chow J.C., Shah J.J and T.G. Pace (1983). The effect of sampling inlets in the PM-10 and PM-15 to TSP concentrations ratios. *Journal of the Air Pollution Control Association* **33(2)**, 114-119.

List of Figures

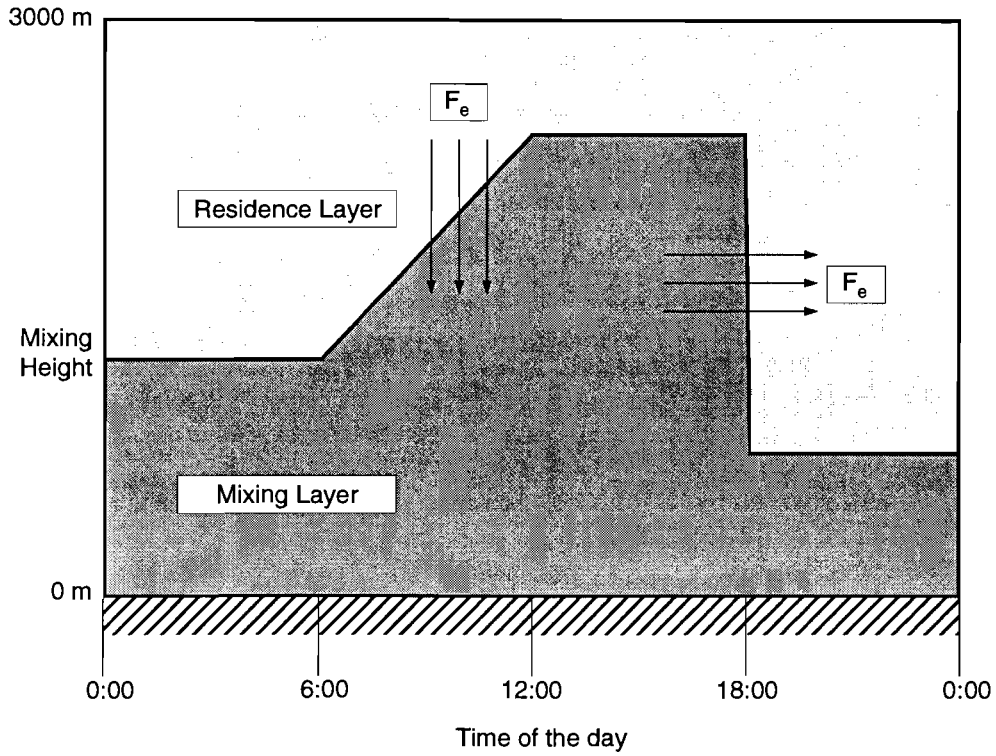

Figure1. Vertical structure of the HMET-50 model.

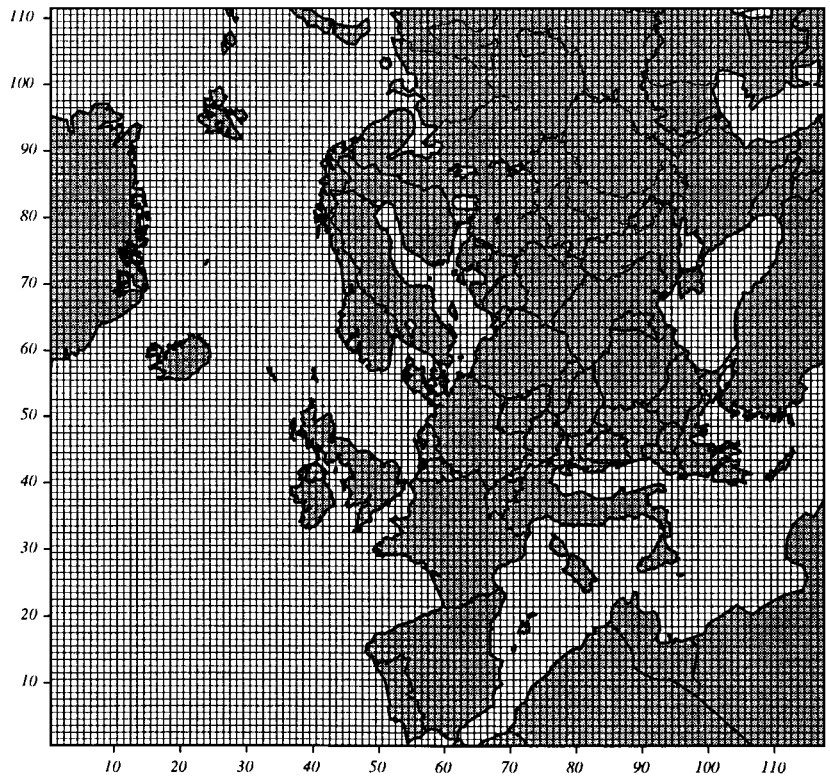

Figure 2. The HMET-50 model domain and the numerical grid system.

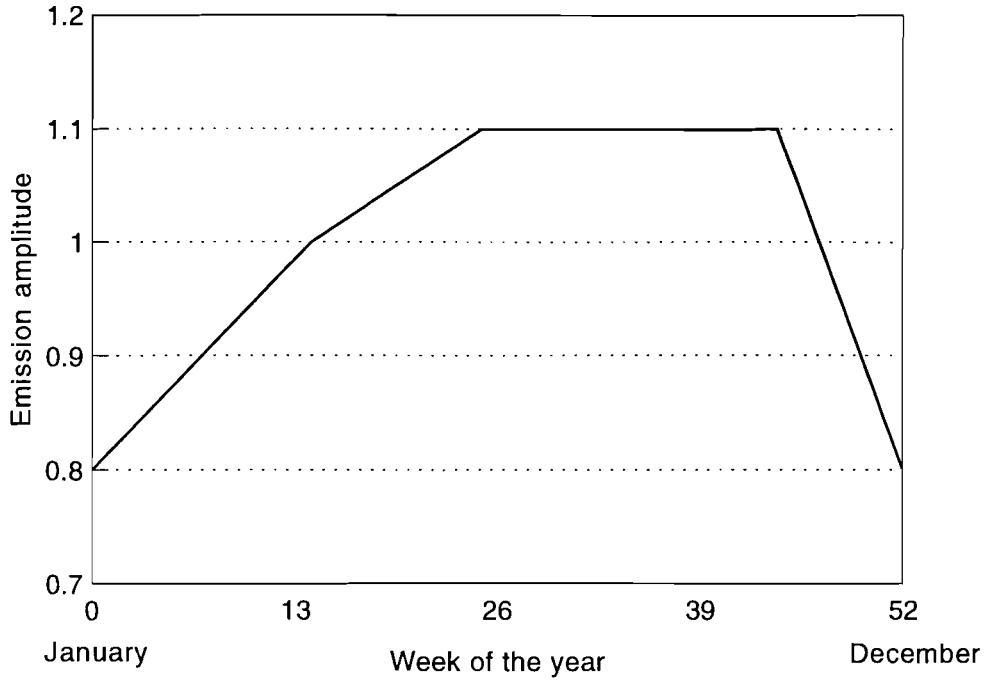

Figure 3. Seasonal pattern of Pb emissions in Europe implemented in the HMET-50 model.

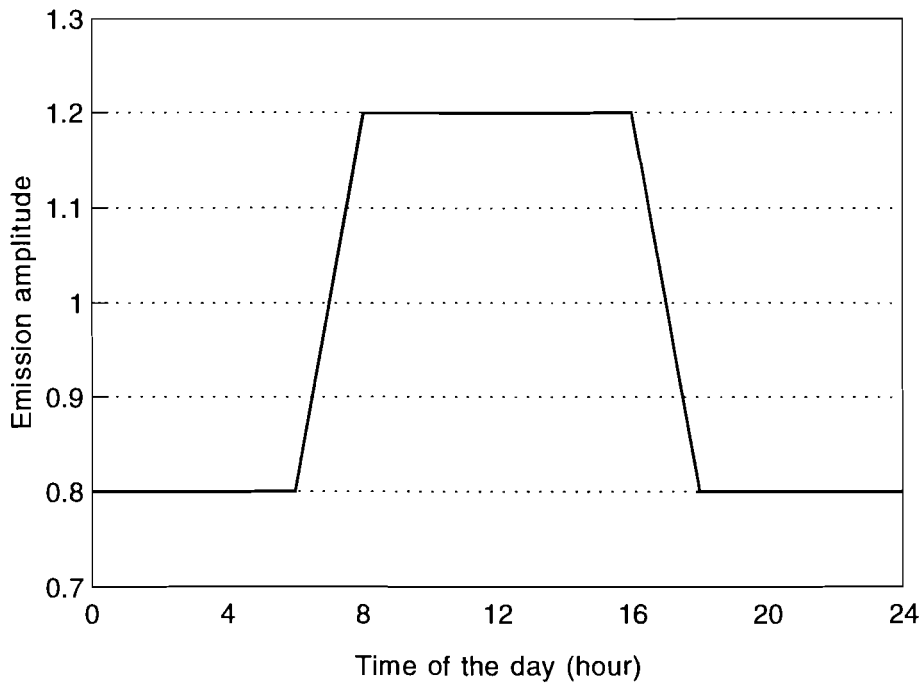

Figure 4. Daily variation of Pb emissions in Europe implemented in the HMET-50 model.

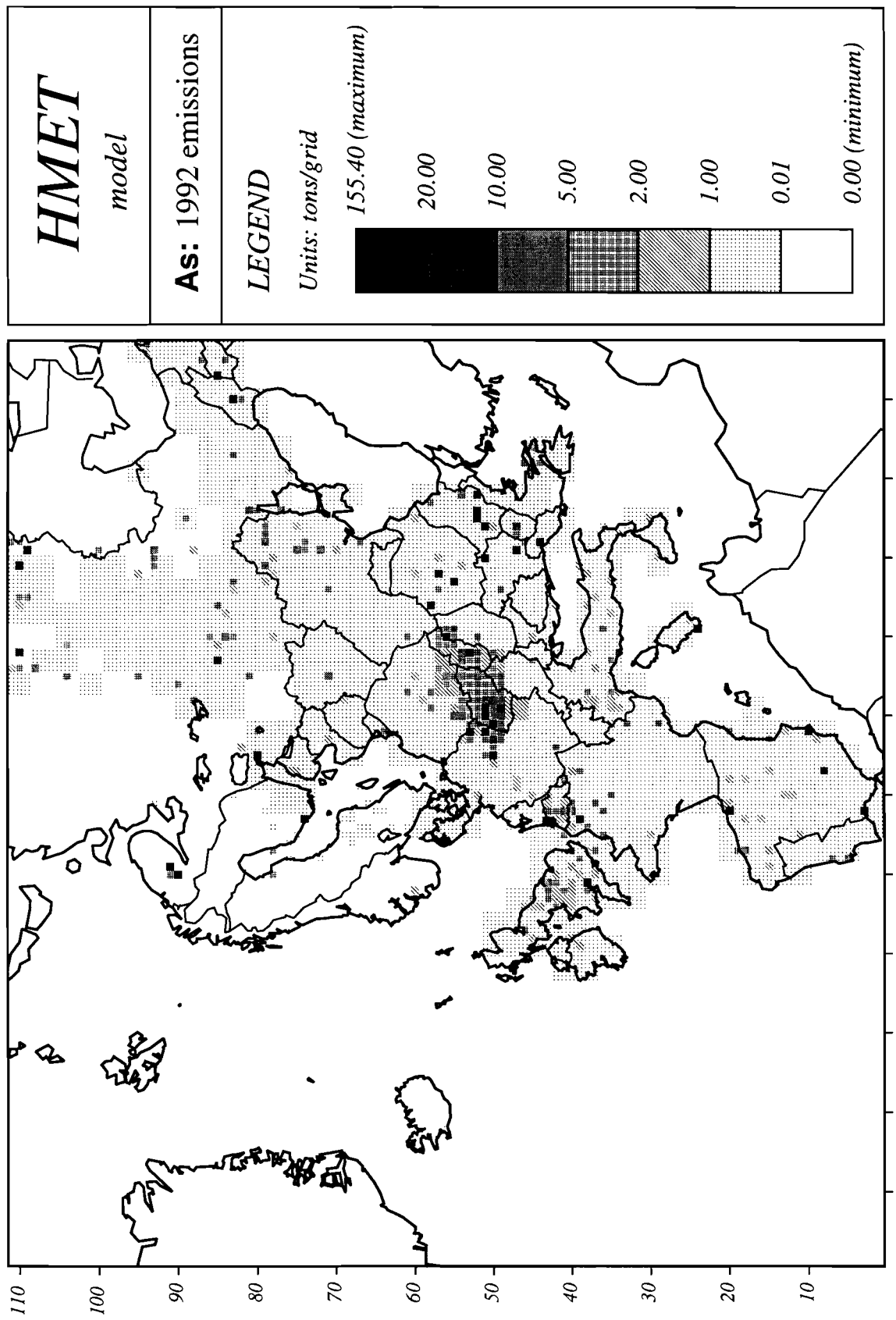

Figure 5. A map of As emissions in Europe in 1992 in the HMET-50 model domain.

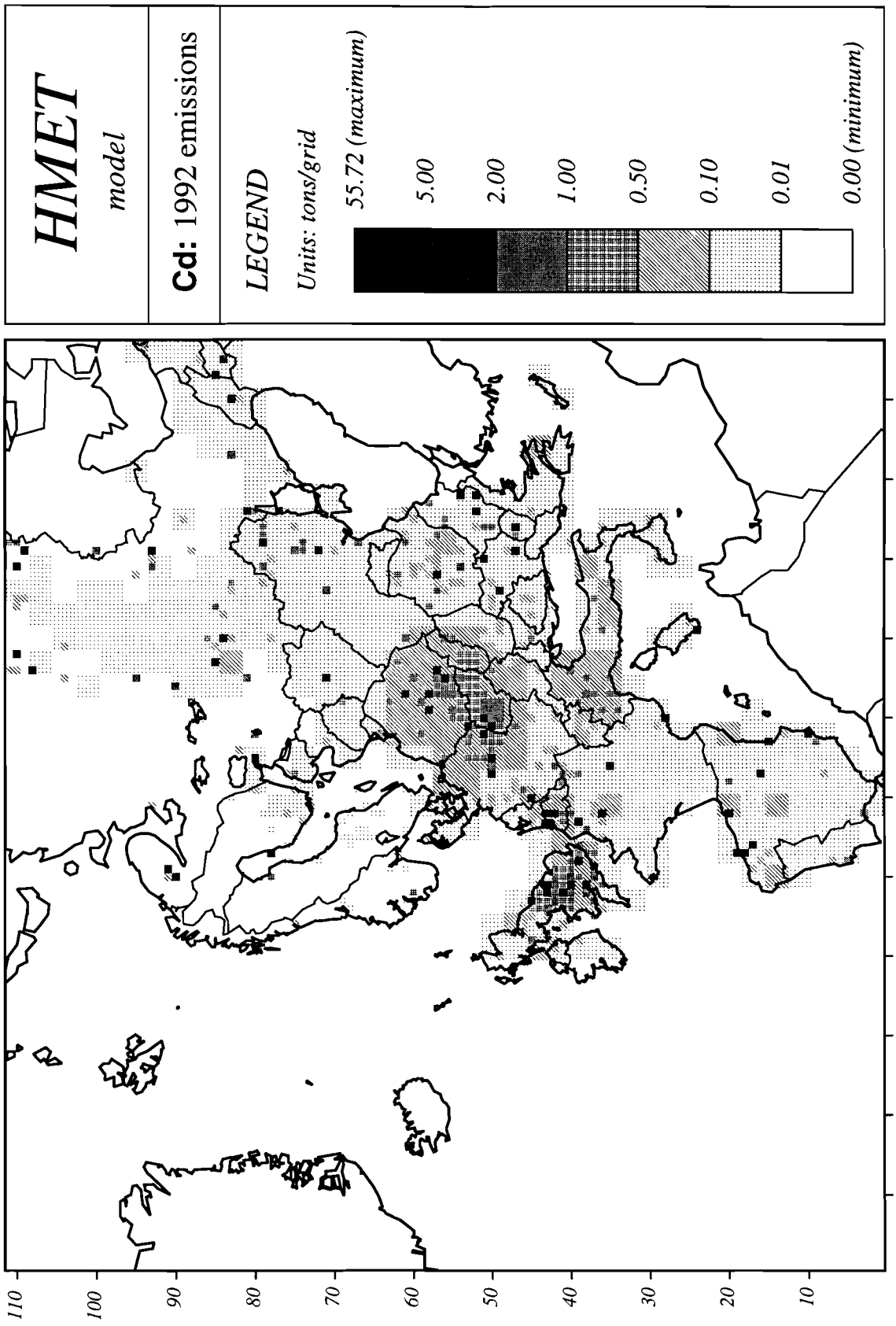

Figure 6. A map of Cd emissions in Europe in 1992 in the HMET-50 model domain.

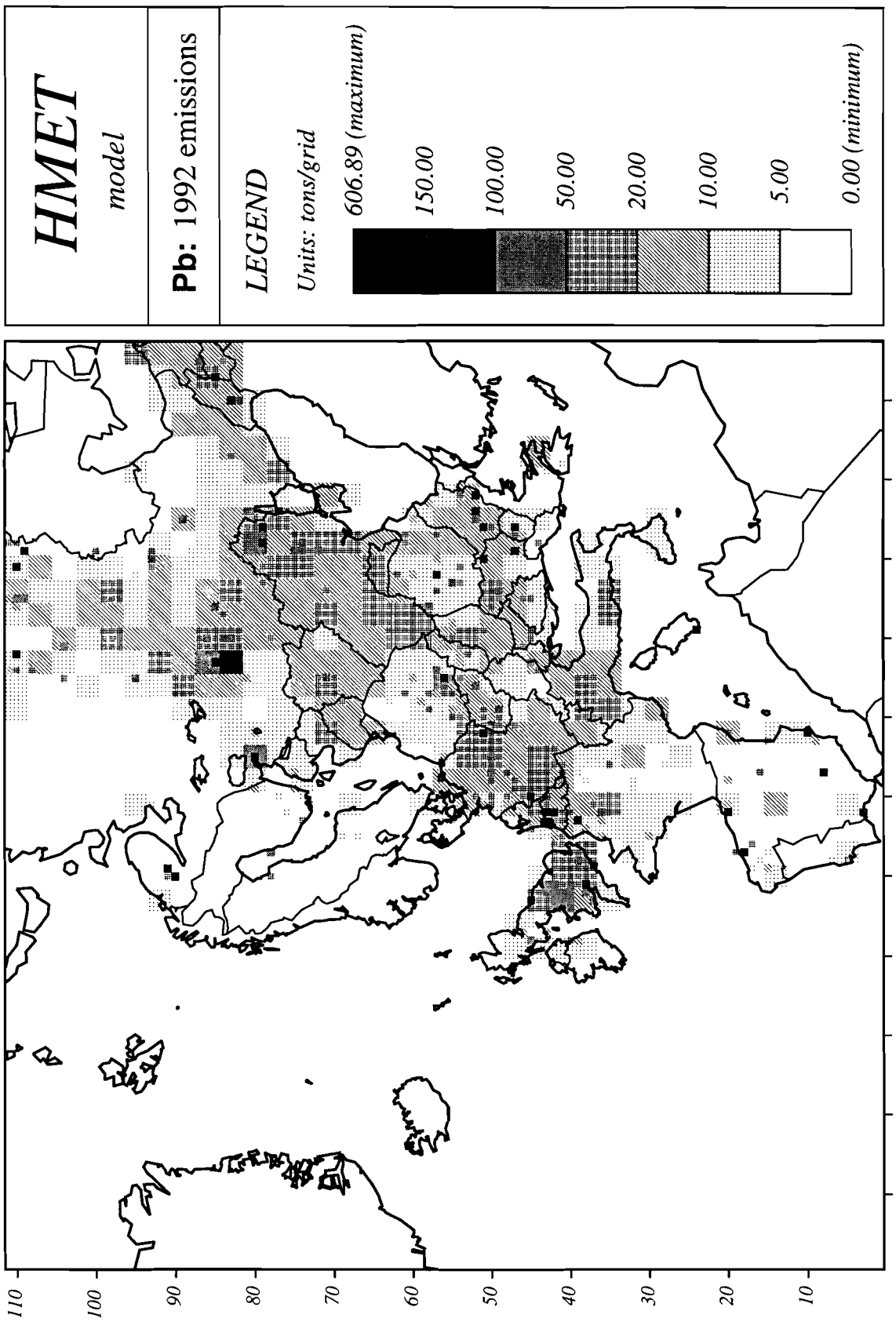

Figure 7. A map of Pb emissions in Europe in 1992 in the HMET-50 model domain.

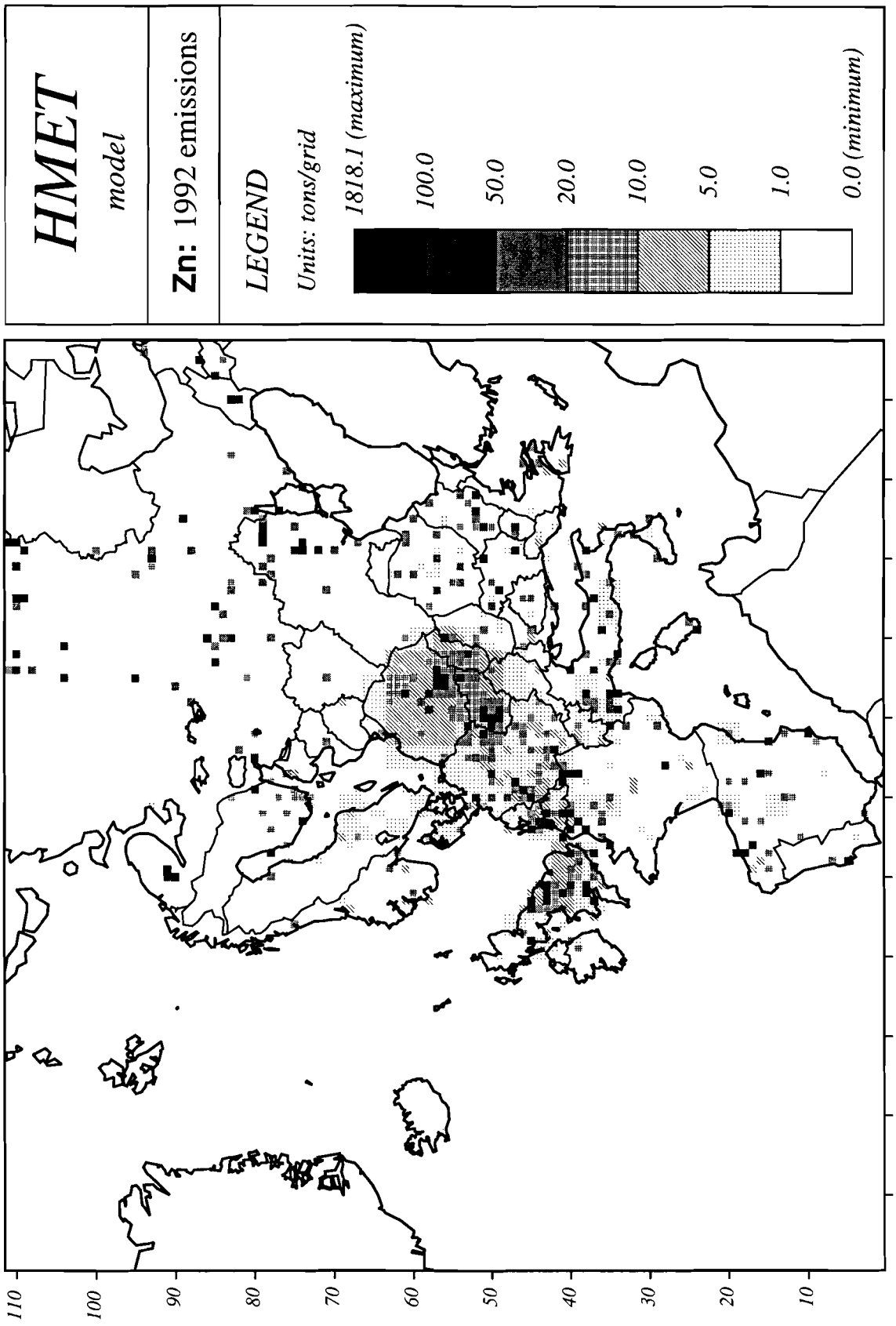

Figure 8. A map of Zn emissions in Europe in 1992 in the HMET-50 model domain.

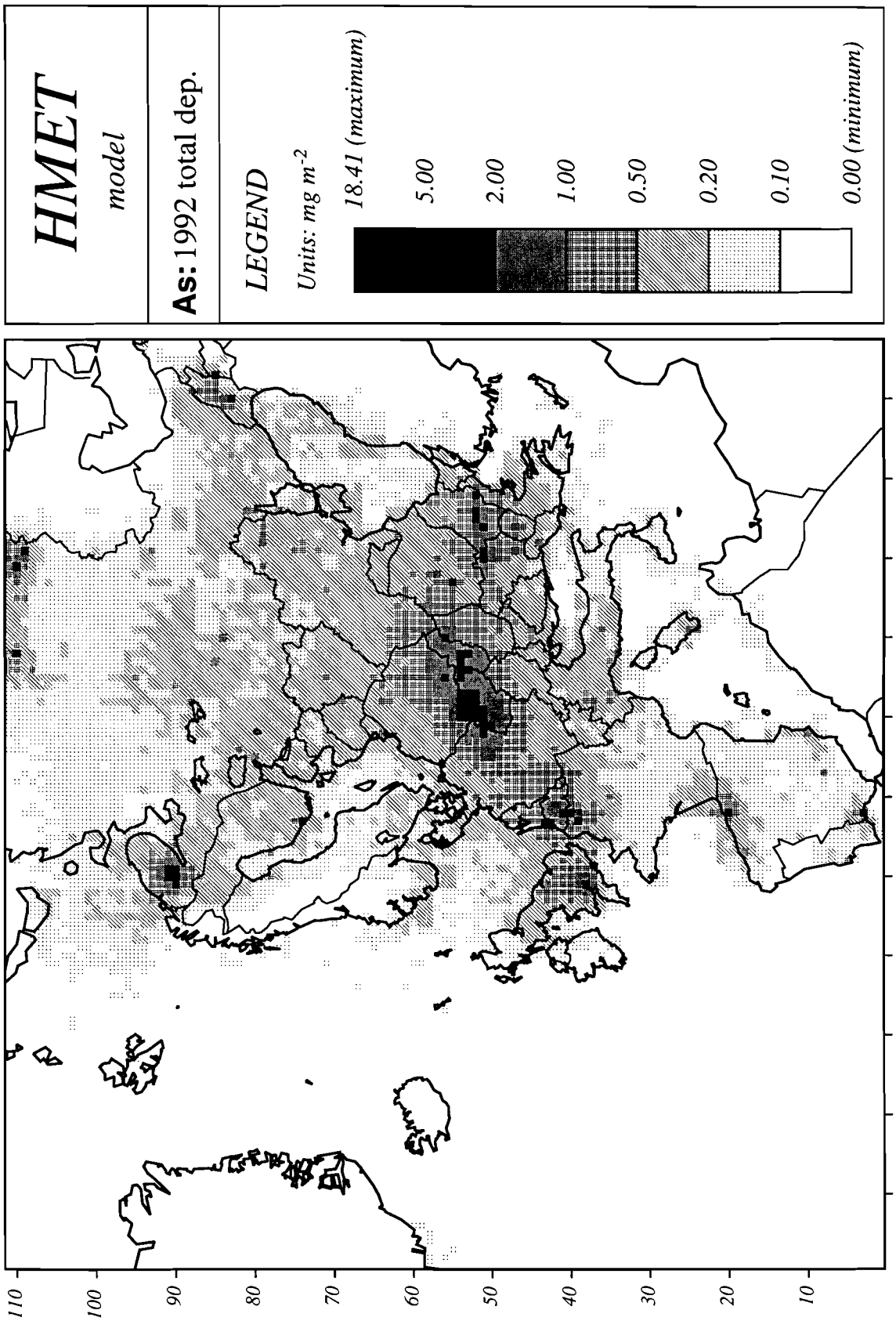

Figure 9. A map of computed annual total deposition of As in Europe in 1992.

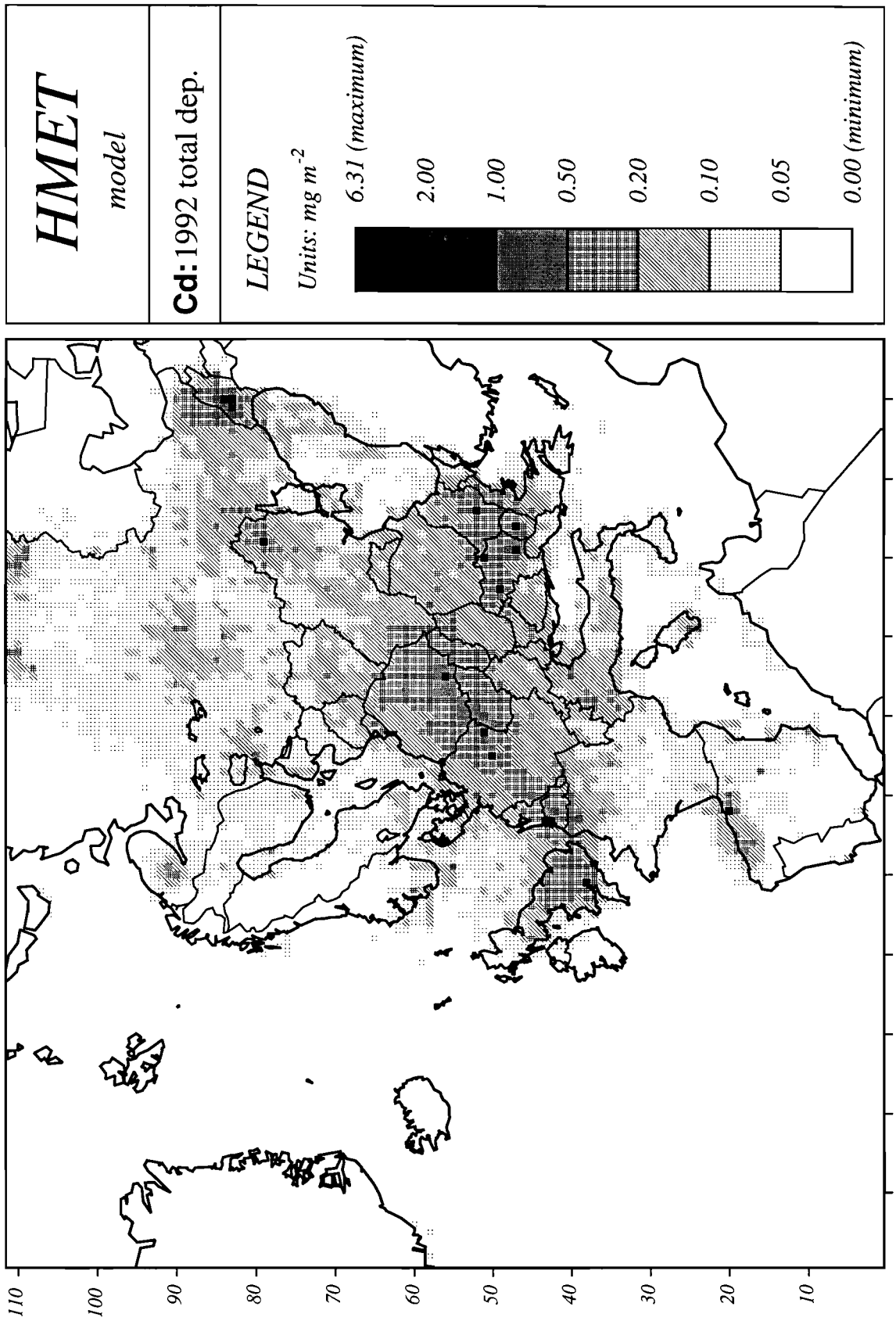

Figure 10. A map of computed annual total deposition of Cd in Europe in 1992.

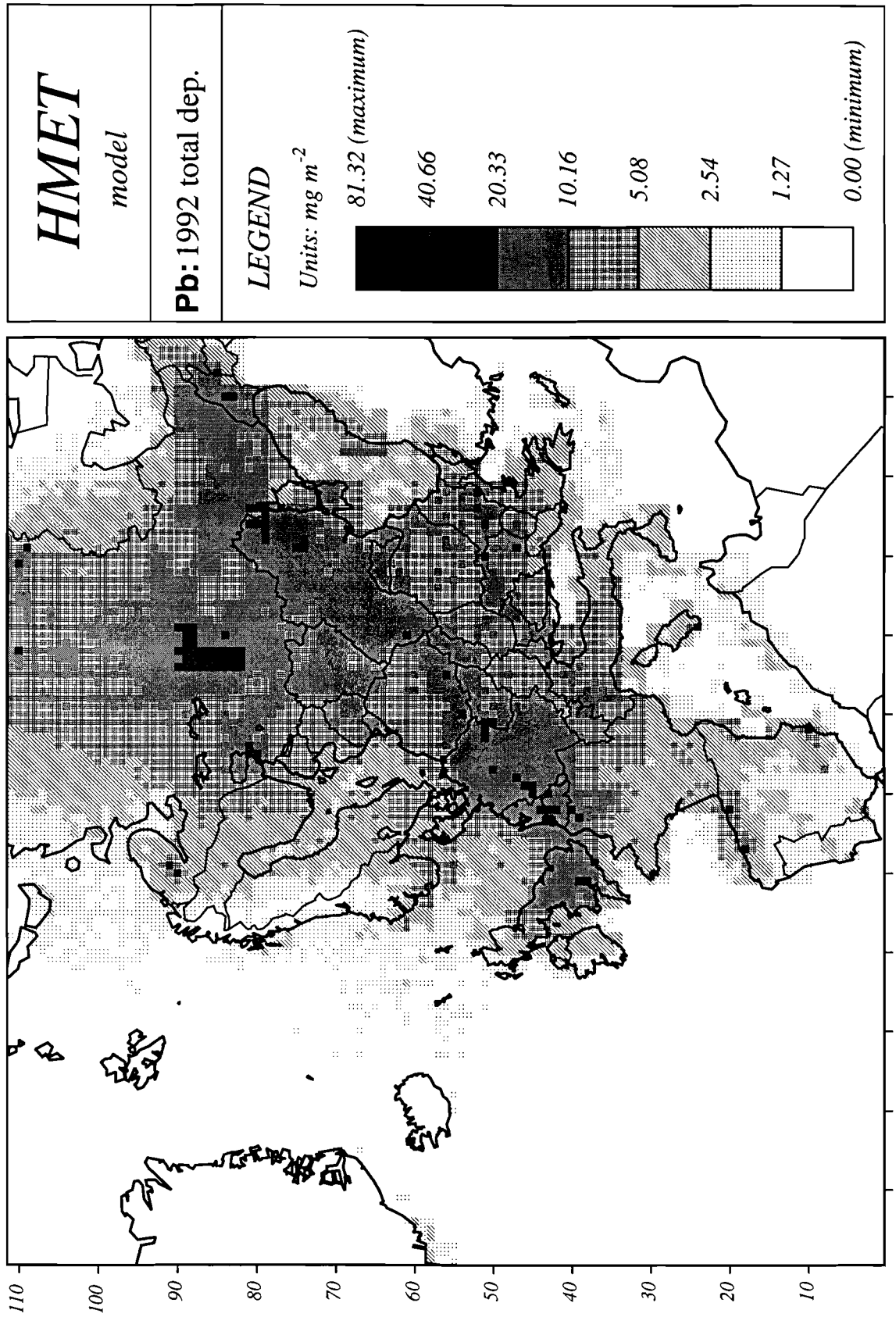

Figure 11. A map of computed annual total deposition of Pb in Europe in 1992.

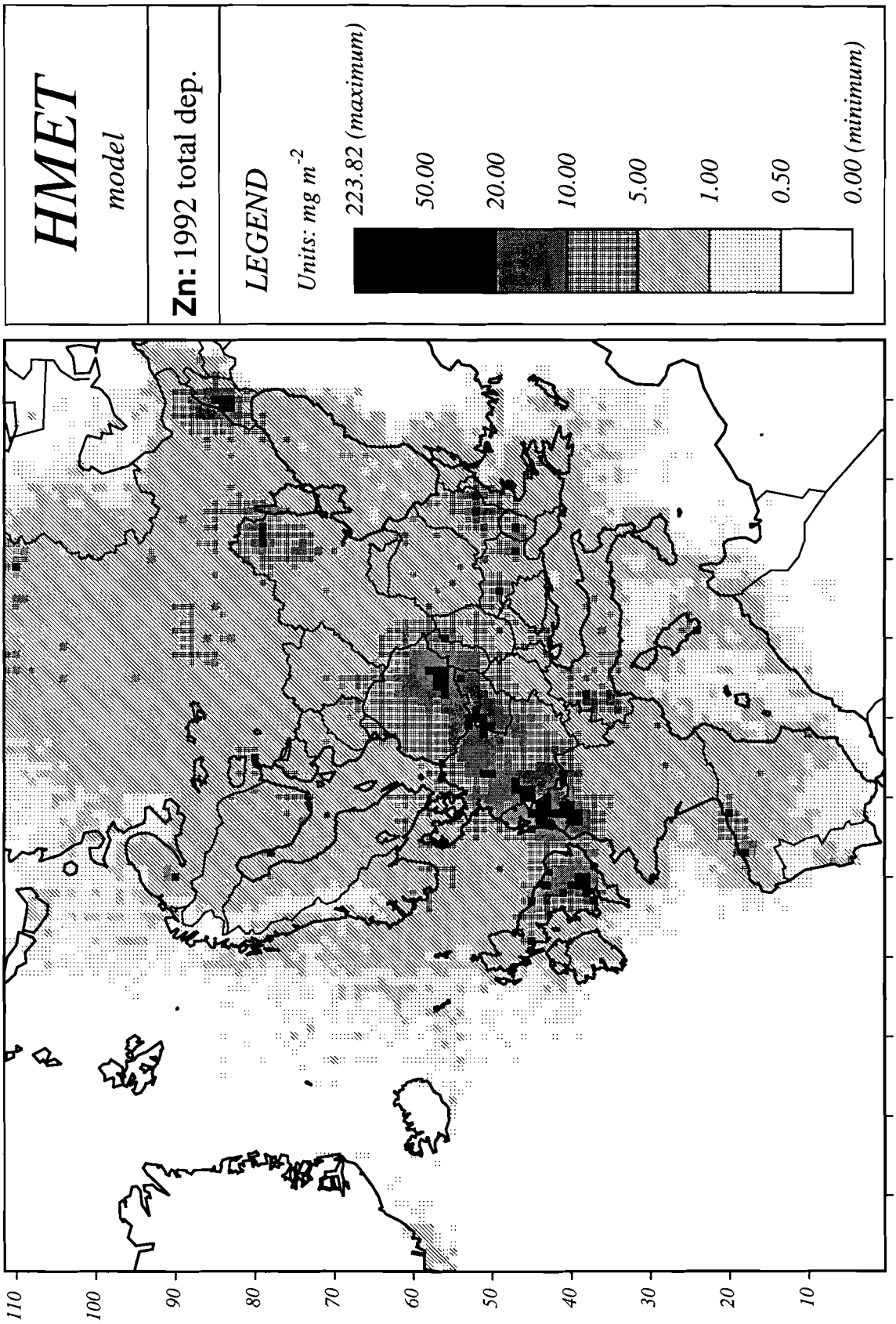

Figure 12. A map of computed annual total deposition of Zn in Europe in 1992.

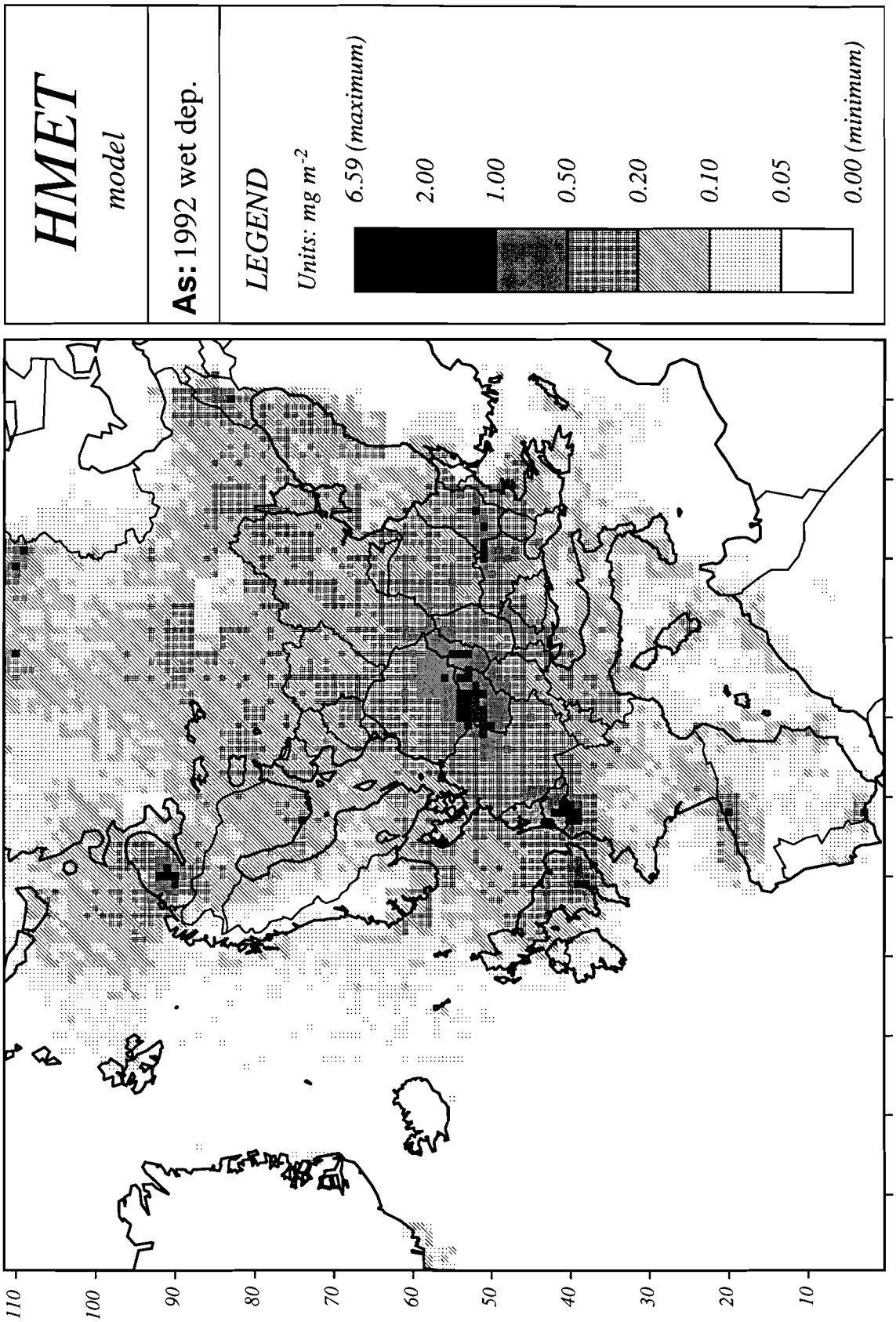

Figure 13. A map of computed annual wet deposition of As in Europe in 1992.

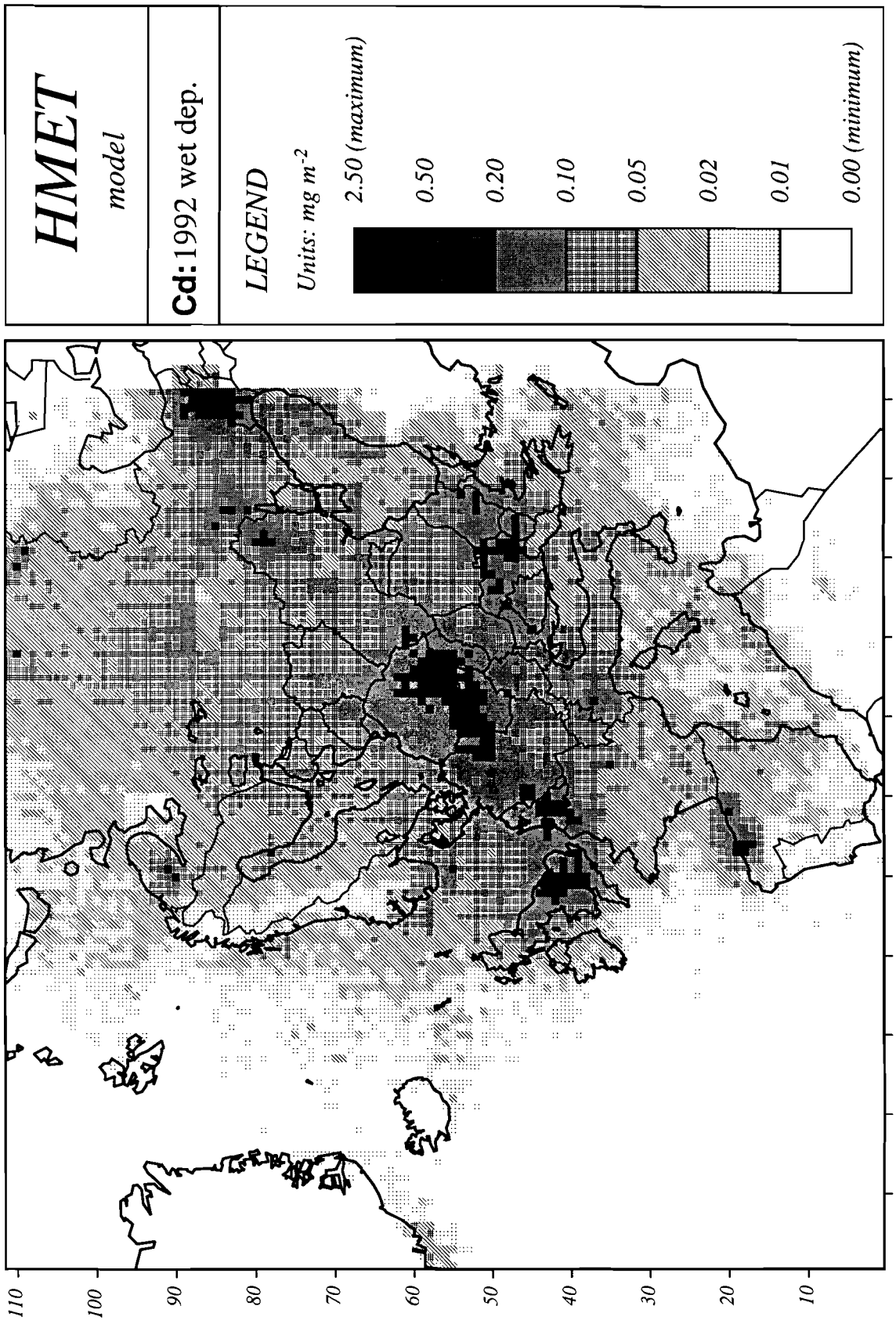

Figure 14. A map of computed annual wet deposition of Cd in Europe in 1992.

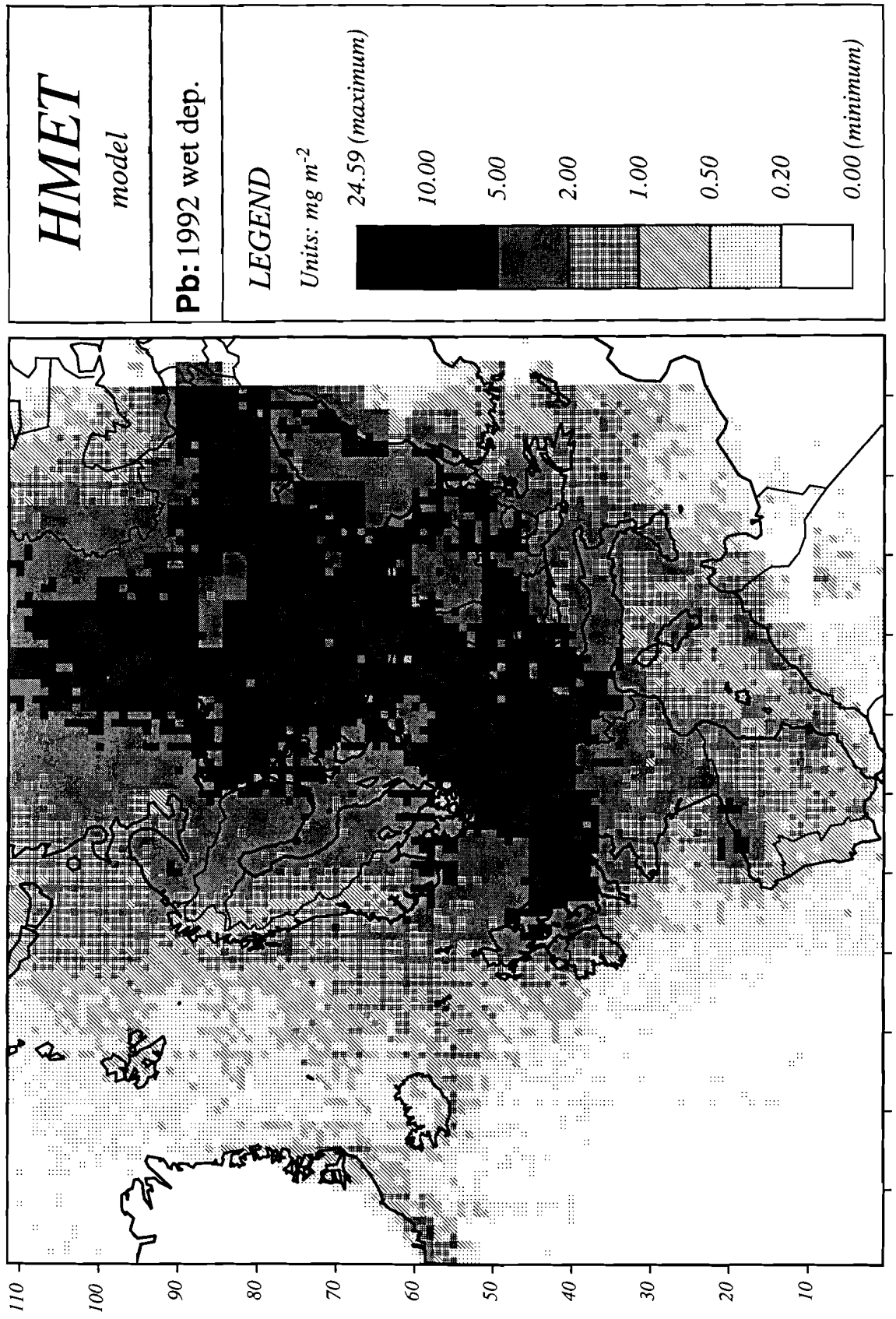

Figure 15. A map of computed annual wet deposition of Pb in Europe in 1992.

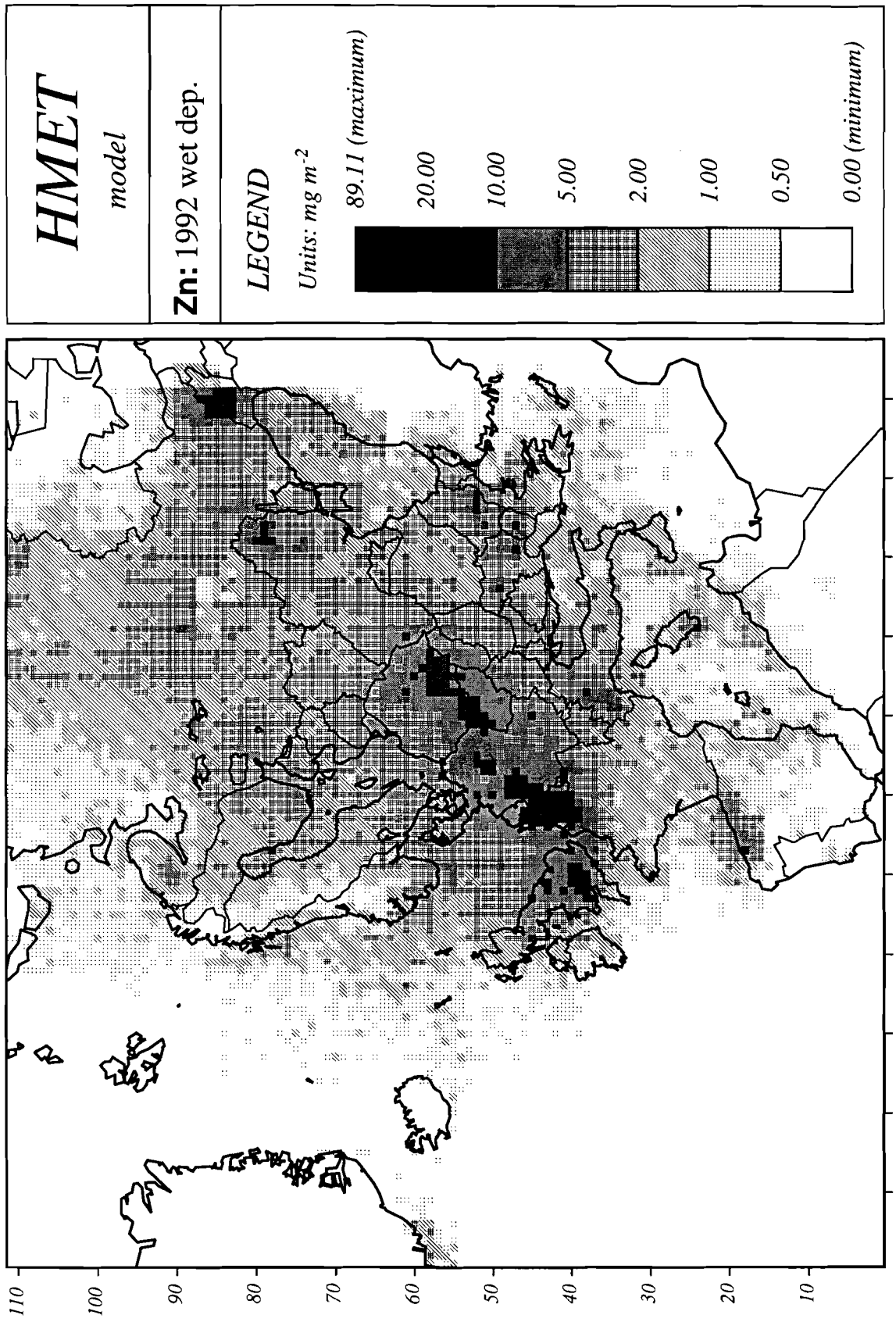

Figure 16. A map of computed annual wet deposition of Zn in Europe in 1992.

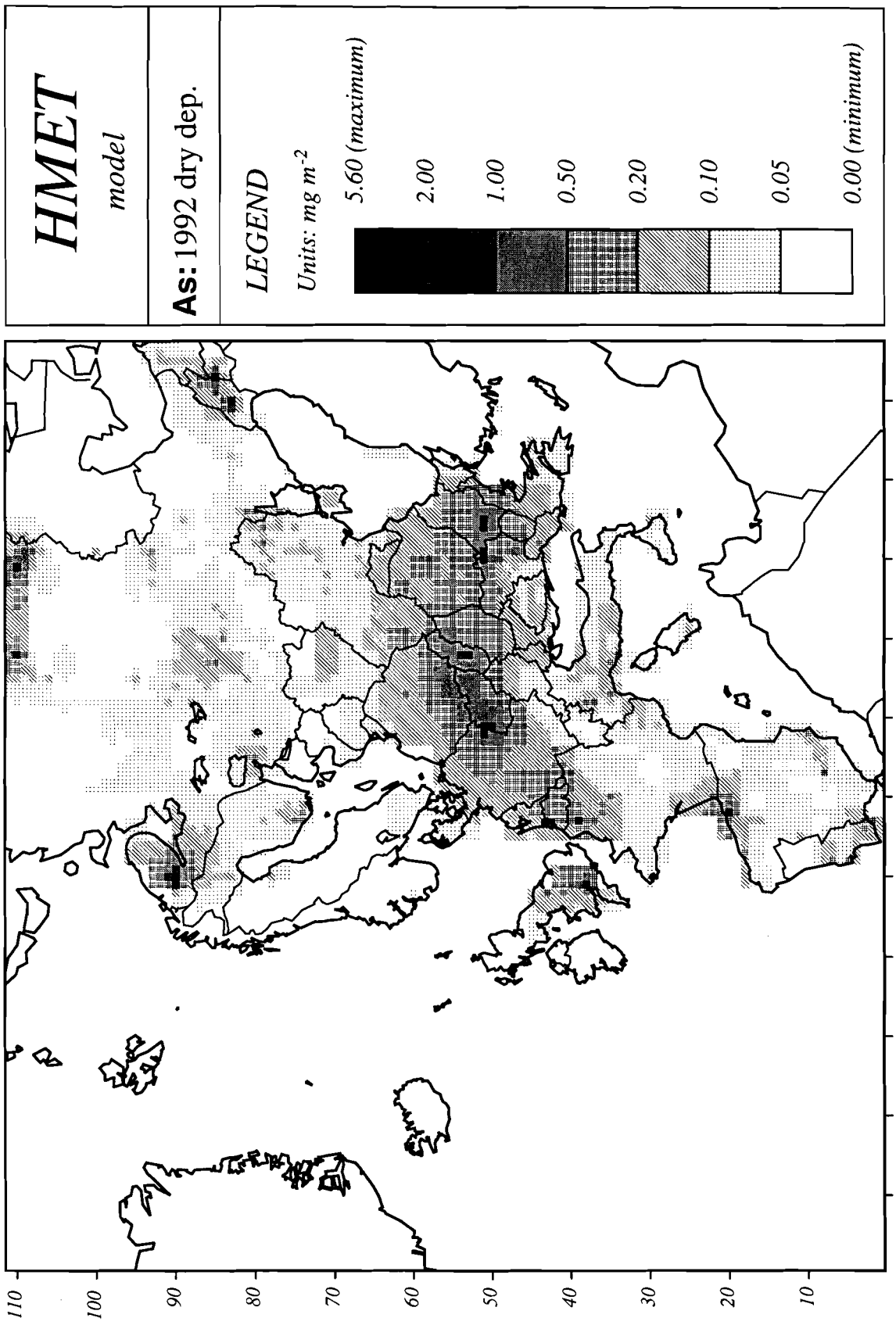

Figure 17: A map of computed dry deposition of As in Europe in 1992.

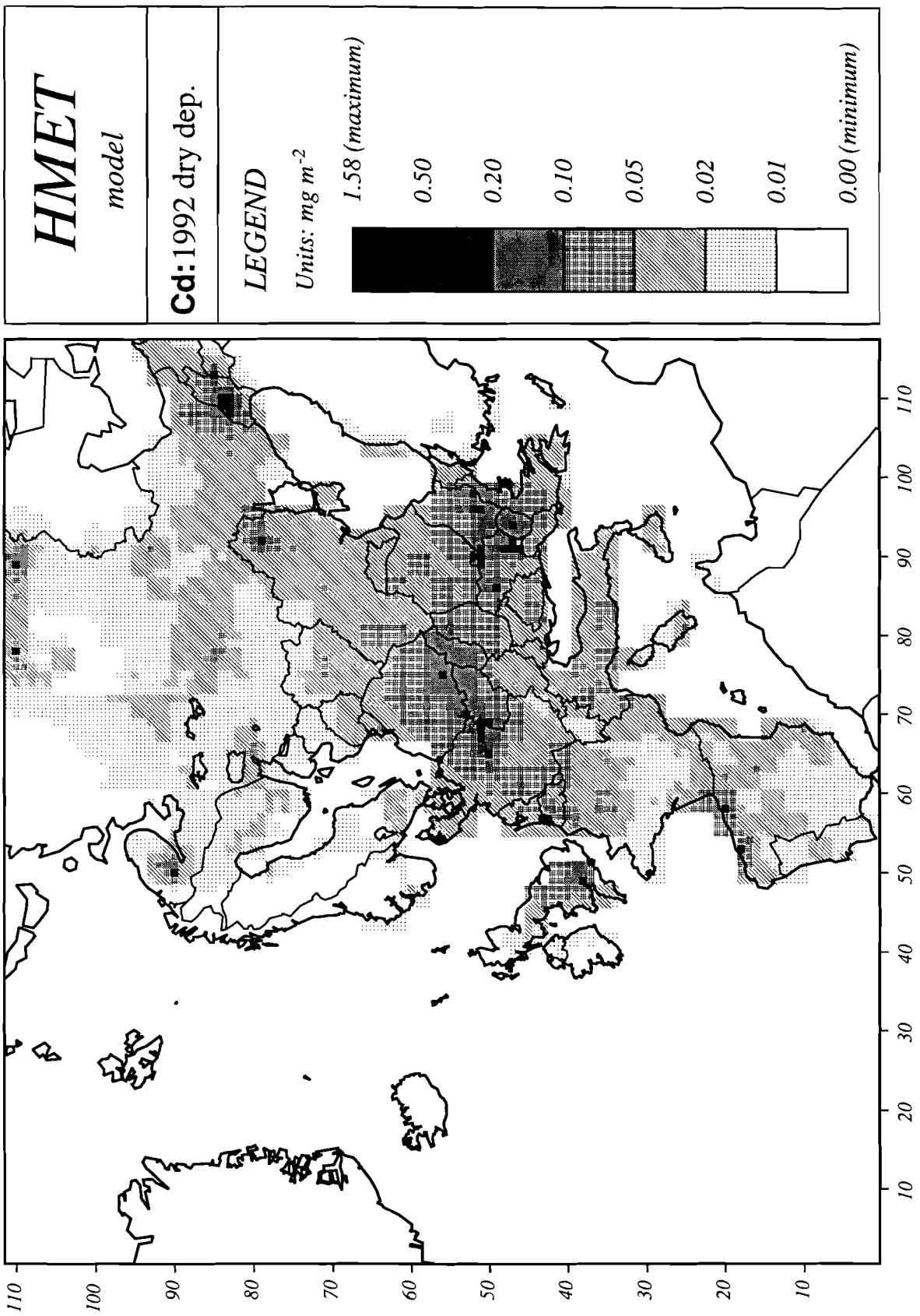

Figure 18: A map of computed dry deposition of Cd in Europe in 1992.

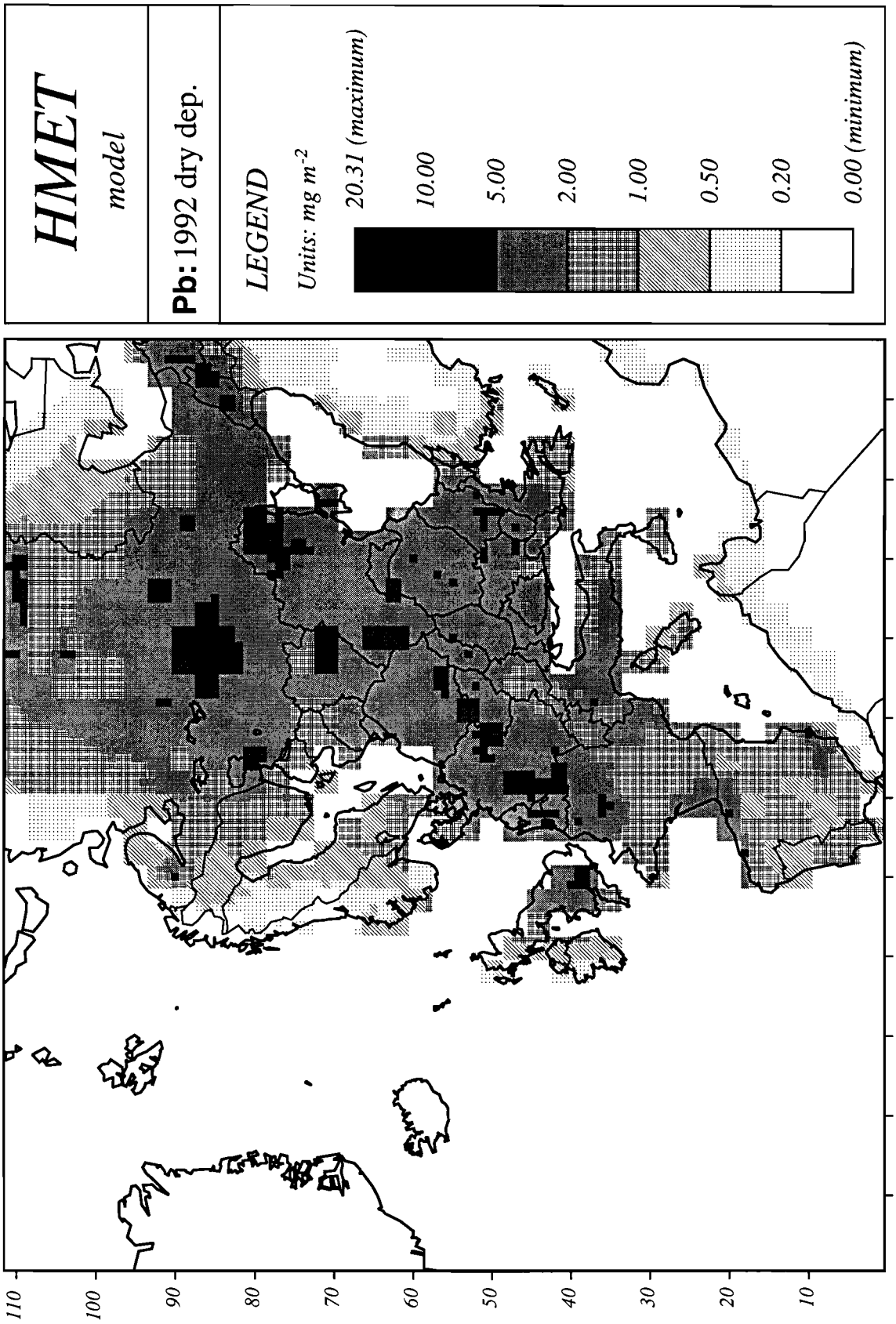

Figure 19: A map of computed dry deposition of Pb in Europe in 1992.

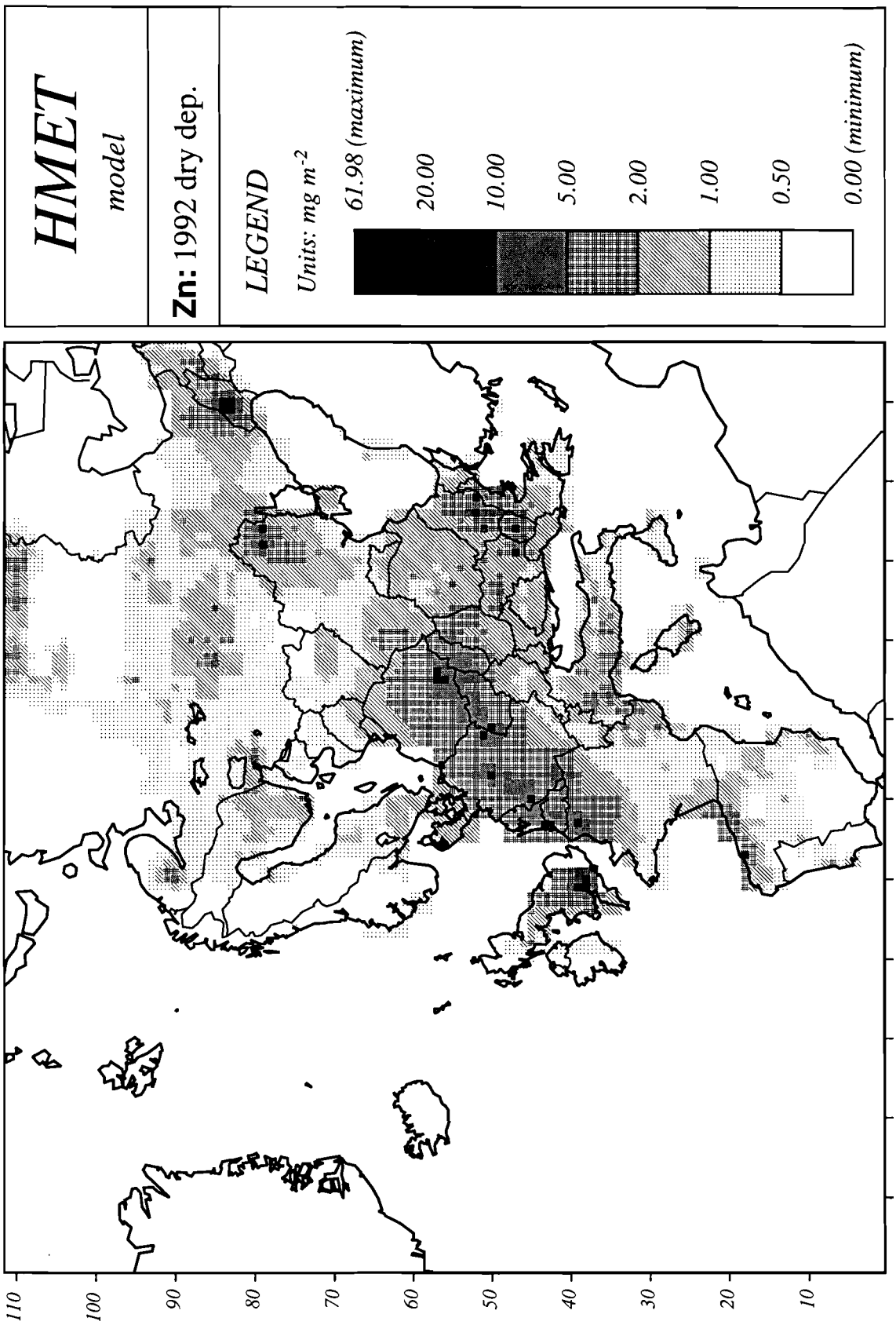

Figure 20: A map of computed dry deposition of Zn in Europe in 1992.

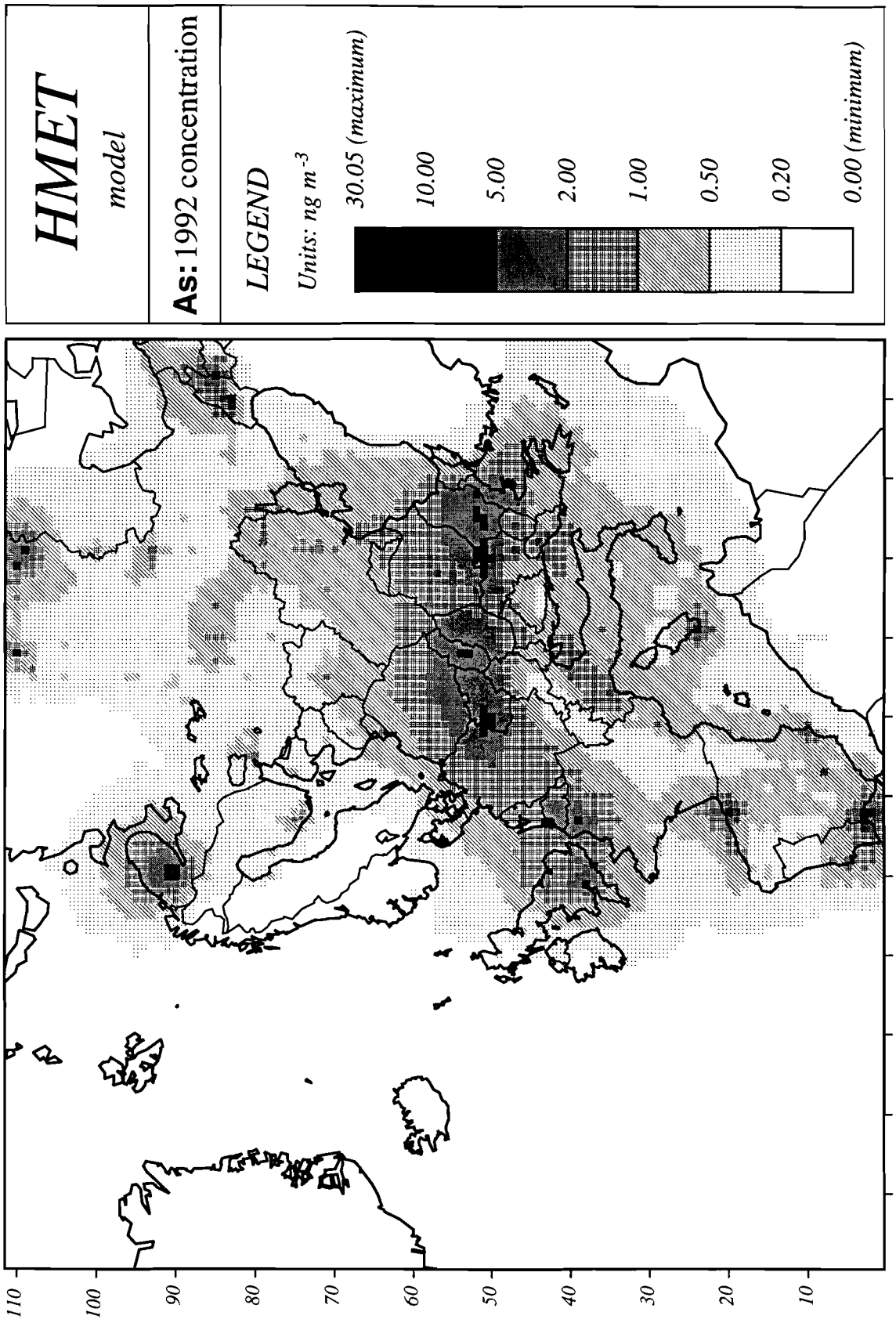

Figure 21. A map of computed mean annual concentration for As in Europe in 1992.

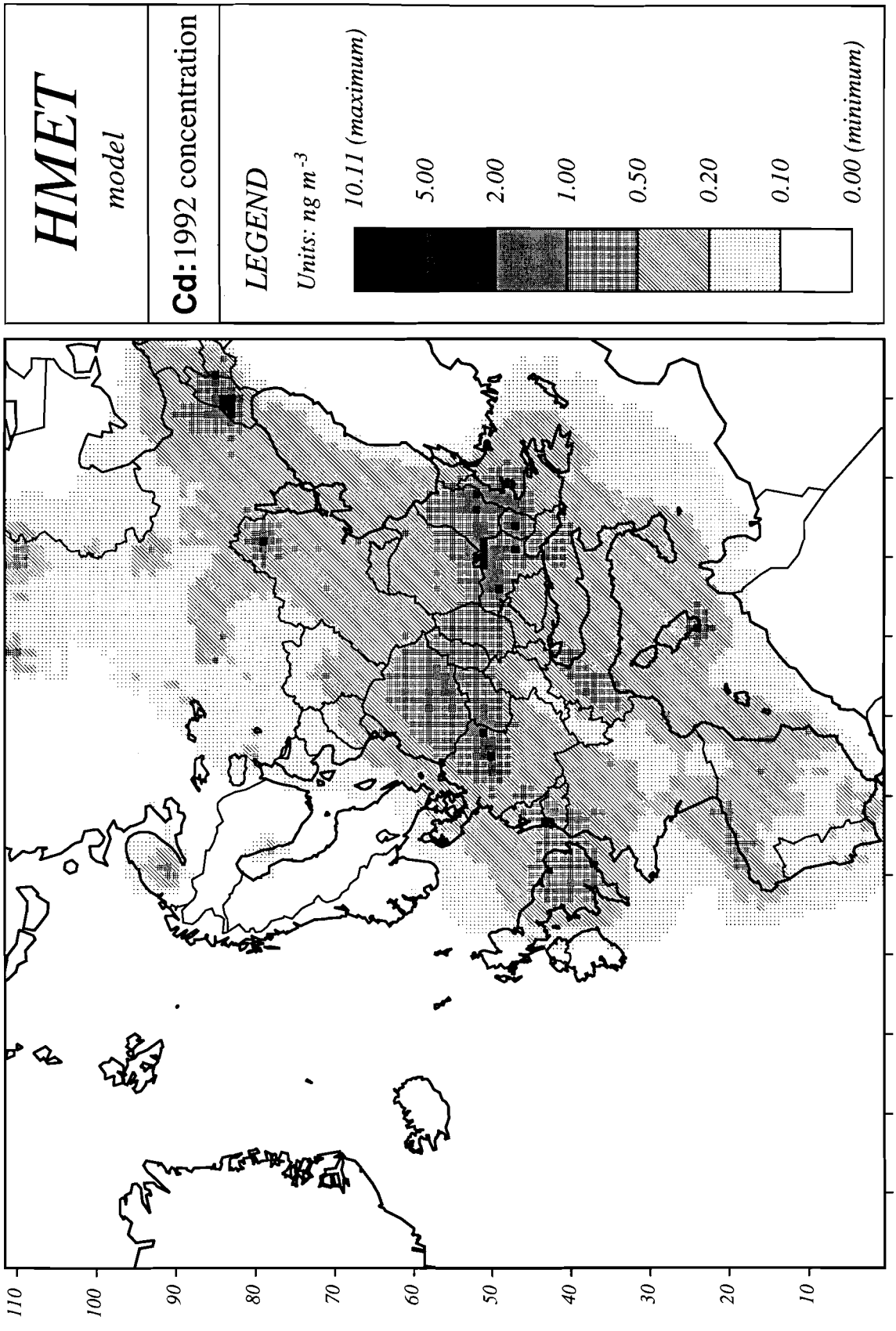

Figure 22. A map of computed mean annual concentration for Cd in Europe in 1992.

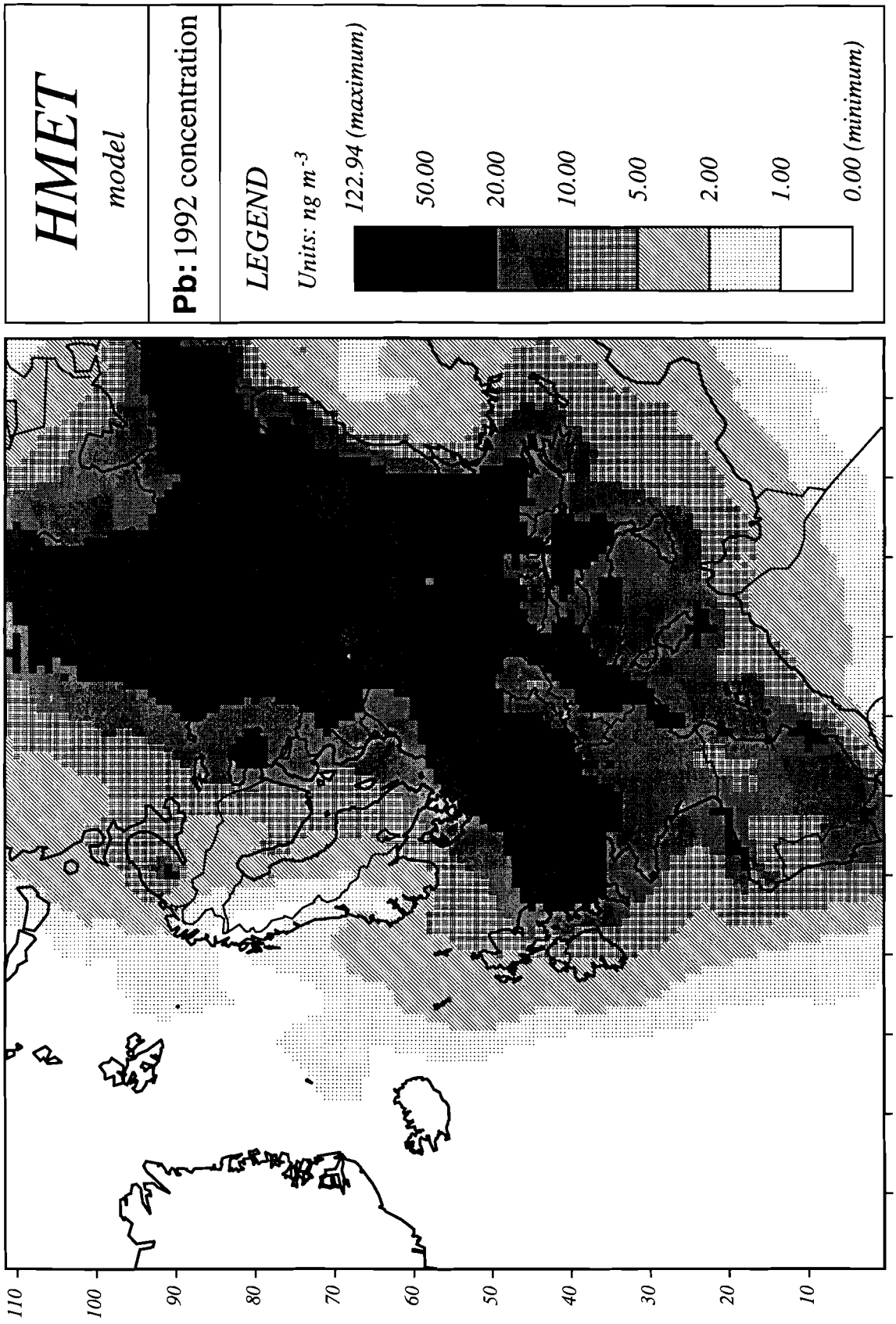

Figure 23. A map of computed mean annual concentration for Pb in Europe in 1992.

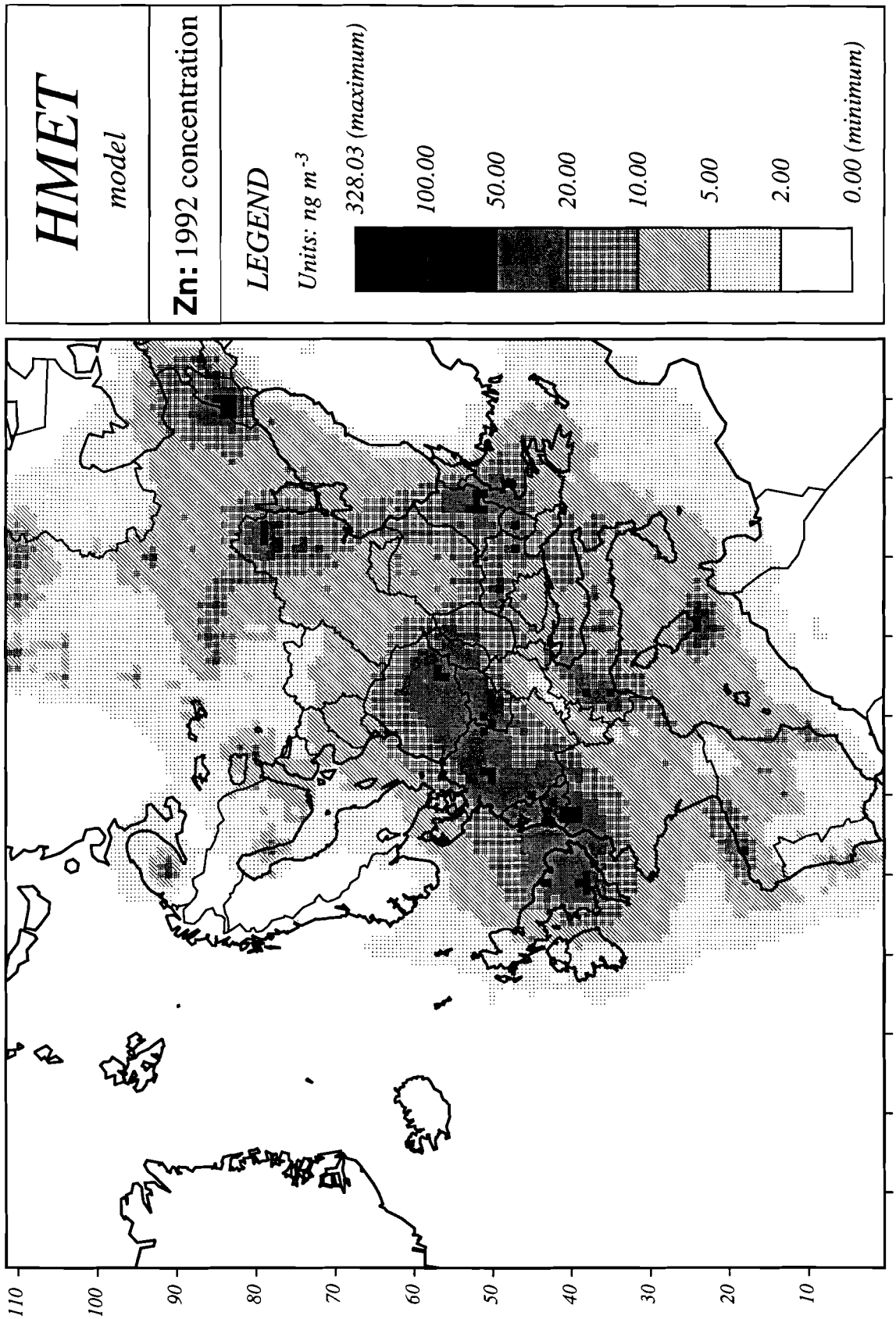

Figure 24. A map of computed mean annual concentration for Zn in Europe in 1992.